

**Determining the effect of lipid nanoemulsions on
insulin signaling and the inflammatory pathways at
the Blood-Brain Barrier**

A Dissertation

SUBMITTED TO THE FACULTY OF THE
UNIVERSITY OF MINNESOTA

BY

Sanjana Suresh Nair

IN PARTIAL FULFILLMENT OF THE
REQUIREMENTS FOR THE DEGREE OF
MASTER OF SCIENCE

Karunya K. Kandimalla

January 2022

Acknowledgments

I'd like to start by thanking my supervisor, Dr. Karunya Kandimalla, who has been a constant source of support and for his help in developing the study topics and methodology. His insightful feedback pushed me to sharpen my insights and brought my work to a higher level. I would like to acknowledge Dr. Timothy Wiedmann and Dr. Ling Li for taking out time from their busy schedule to be on my thesis committee and for providing their valuable feedback on my dissertation.

I'd like to thank my lab mates Lushan Wang, Vrishali Salian, Zengtao Wang, Chenxu Li, and Andrew Zhou for their continued input and support during my study; they gave me the tools I needed to take the appropriate path and finish my dissertation effectively. I'd want to thank my Lab mate Lushan Wang in particular for her patience and for all of the possibilities she has provided me to pursue my research.

In addition, I'd want to express my gratitude to my parents for their sound advice and sympathetic ear. Finally, I could not have finished this dissertation without the help of my closest friends, Dharamveer Kumar, Srishti Shetty, Nikita Nair, Ashika Jain, and Tvisha Shah, who provided me company during the late-night experiments as well as delightful distractions to rest my mind outside of my research.

TABLE OF CONTENTS

List of table	iv
List of figures	iv
Abstract	vii
1.0 Introduction	
1.1 Alzheimer's disease (AD)	
1.1.1 Alzheimer's disease and dementia.....	1
1.1.2 Stages of Alzheimer's disease.....	3
1.2 Blood-Brain Barrier (BBB)	
1.2.1 Blood-Brain Barrier- structure, functions, and role in AD.....	3
1.2.2 Blood-Brain Barrier dysfunction.....	7
1.2.3 Role of lipids dysfunction in AD.....	8
1.3 Insulin resistance and inflammation	
1.3.1 Insulin resistance.....	9
1.3.2 Inflammation.....	11
1.4 Delivery across the BBB	
1.4.1 Nanoparticles.....	12
1.4.2 Nanoemulsions.....	13
1.4.3 Formulation of nanoemulsion.....	14
1.5 Current treatments.....	17
2.0 Statement of the problem	
2.1 Statement of problem.....	18
2.2 Specific aims.....	21
3.0 Materials and Methods	
3.1 Nanoemulsion formulation and characterization	
3.1.1 Materials.....	22
3.1.2 Nanoemulsion Formulation.....	22
3.1.3 Nanoemulsion characterization.....	24

3.2 Cell culture.....	25
3.3 Western blot.....	25
3.4 Antibody and protocol optimization for confocal microscopy.....	26
3.5 Confocal microscopy.....	26
3.6 Statistical Analysis.....	27
4.0 Results	
4.1 Particle size and zeta potential of the nanoemulsion.....	28
4.2 Effect of TNF- α on insulin resistance and inflammation in BBB endothelial cells	
4.2.1 Time-dependent effect of TNF- α exposure.....	29
4.2.2 Antibody and protocol optimization for confocal microscopy.....	30
4.3 Effect of TNF- α and nanoemulsion (CNEs & SNEs) on insulin signaling and VCAM-1 expression.....	32
4.4 Insulin resistance and VCAM-1 expression in the presence of A β -42 and nanoemulsions.....	35
4.5 Effect of TNF- α and FNEs on insulin signaling and VCAM-1 expression.....	40
5.0 Discussion	42
6.0 Conclusion and Future plans	
6.1 Conclusion.....	46
6.2 Future plans.....	47
7.0 Bibliography	48

List of tables:

Table 1: Summary of fatty acids in Coconut, Soybean, and Fish oil.....19

List of figures:

Figure 1: Schematic representation of the Blood-Brain Barrier.....4

Figure 2: Structure of 1,2-dioleoyl-3-trimethylammonium-propane (DOTAP) as a chloride salt.....15

Figure 3: Structure of 1,2-dioleoyl-3-trimethylammonium-propane (DOTAP) as a chloride salt.....15

Figure 4: Schematic representation of lipid nanoemulsions.....16

Figure 5: Diagrammatic representation of TNF- α mediated VCAM-1 expression and PI3K pathway inhibition.....20

Figure 6: Diagrammatic representation of formulating soybean oil (SNEs) and coconut oil (CNEs) nanoemulsions.....23

Figure 7: (A) Summary of particle characterization of various nanoemulsions (B) particle size analysis using NanoSight.....28

Figure 8: (A) Western blots showing the expression of p-AKT and AKT with and without TNF- α exposure. (B) Quantitation of p-AKT/AKT ratios (C) Western blots showing the time-dependent effect of TNF- α on VCAM-1 expression (D) Fold change in VCAM-1 expression with various treatments (One-way ANOVA with Tukey's post-tests, **p<0.01 and ***p<0.001).....29

Figure 9: Confocal images of VCAM-1 expression detected by immunocytochemistry using two different primary antibodies and permeabilization methods. (A) Cells incubated with 1:1000 AF-647 labeled goat anti-rabbit IgG (secondary antibody) and permeabilized with methanol (B) Cells treated with TNF- α and 1:250 VCAM-1 primary antibody (Abcam, Waltham, MA 02453) and

secondary antibody followed by permeabilization with methanol (C) Cells treated with TNF- α and 1:250 VCAM-1 P3C4 primary antibody (Developmental Studies Hybridoma Bank, The University of Iowa, Iowa City, IA) and secondary antibody followed by permeabilization with methanol (D) Cells incubated with secondary antibody alone, fixed with 4% paraformaldehyde (PFA), and permeabilized with 0.1% Triton-X (E) Cells treated with TNF- α and 1:250 VCAM-1 primary antibody (Abcam, Waltham, MA 02453) and secondary antibody, fixed with 4%PFA, and permeabilized with 0.1% Triton-X (F) Cells treated with TNF- α and 1:250 VCAM-1 P3C4 primary antibody (Developmental Studies Hybridoma Bank, The University of Iowa, Iowa City, IA) and secondary antibody, fixed with 4%PFA, and permeabilized with 0.1% Triton-X.....31

Figure 10: (A) Western blot showing the effect of CNEs on p-AKT and AKT after the cells were exposed to TNF- α and Humulin® (B) Quantitation p-AKT/AKT ratios after cells were treated with CNEs, TNF- α and Humulin® (C) Western blot showing the effect of SNEs on p-AKT and AKT after the cells were exposed to TNF- α and Humulin® (D) Quantitation p-AKT/AKT ratios after cells were treated with SNEs, TNF- α , and Humulin® (One-way ANOVA with Tukey’s post-tests, *P<0.05, **P<0.01, ***p<0.001).....33

Figure 11: Confocal images for determining VCAM-1 expression upon exposure to various nanoemulsions, TNF- α , and Humulin®. (A) Secondary antibody control (B) Untreated control (C) Humulin® treatment (D) Cells treated with CNEs (E) Cells treated with SNEs (F) Cells treated with TNF- α (G) TNF- α + Humulin® (H) TNF- α + CNEs (I) TNF- α + SNEs (J) TNF- α + CNEs+ Humulin® (K) TNF- α + SNEs+ Humulin®.....34

Figure 12: (A) Western blots showing the effect of coconut oil nanoemulsions (CNEs) on p-AKT and AKT after the cells were exposed to A β -42 and Humulin® (B) Quantitation of p-AKT/AKT ratio after cells were treated with CNEs, A β -42 and Humulin® (C) Western blots showing the effect of coconut oil nanoemulsions (SNEs) on p-AKT and AKT after the cells were exposed to A β -42 and

Humulin® (D) Quantitation of p-AKT/AKT ratio after cells were treated with SNEs, Aβ-42 and Humulin® (One-way ANOVA with Tukey's post-tests, ****p<0.0001).....37

Figure 13: Confocal images for determining VCAM-1 expression in the presence of nanoemulsions (NEs), Aβ-42, and Humulin®. (A) Secondary Ab control (B) Untreated control (C) Cells treated with Humulin® (D) Cells treated with CNEs (E) Cells treated with SNEs (F) Cells treated with Aβ-42 (G) Aβ-42+ Humulin® (H) Aβ-42+ CNEs (I) Aβ-42+ SNEs (J) Aβ-42+ CNEs+ Humulin® (K) Aβ-42+ SNEs+ Humulin®.....38

Figure 14: VCAM-1 fluorescence intensities were quantified on Image J and presented as mean ± SD (One-way ANOVA with Tukey's post-tests, *P<0.05).....39

Figure 15: (A) Western showing the effect of fish oil nanoemulsions (FNEs) on p-AKT and AKT after the cells were exposed to TNF-α and Humulin® (B) Quantitation of the p-AKT/AKT ratios after cells were treated with FNEs, TNF- α, and Humulin® (One-way ANOVA with Tukey's post-tests, *P<0.05, **P<0.01, ****p<0.0001)40

Figure 16: Confocal images of VCAM-1 expression upon treatment with fish oil nanoemulsions (FNEs), TNF-α, and Humulin®. (A) Secondary Ab control (B) Untreated control (C) Cells treated with Humulin® (D) Cells treated with FNEs (E) Cells treated with TNF-α (F) TNF-α+ Humulin® (G) TNF-α+ FNEs (H) TNF-α+ FNEs+ Humulin® (I) Quantification of VCAM-1 fluorescence intensities by Image J and analyzed using GraphPad Prism.....42

Abstract:

Several studies have shown that metabolic disorders such as type-2 diabetes (T2DM) play a role in propagating neurodegenerative disorders like Alzheimer's Disease (AD)(1). As the brain is an insulin-sensitive organ and requires insulin for promoting neuronal integrity and function, impairment of insulin signaling in the CNS has huge implications for memory and cognition(2). Hyperinsulinemia observed in AD and T2DM contributes to vascular inflammation, which in turn, leads to endothelial insulin resistance by impairing insulin receptor (IR) and insulin resistance substrate (IRS)-1(1). The insulin resistance leads to a compensatory increase in circulating insulin leading to hyperinsulinemia. In addition to the impairment of insulin signaling, another hallmark of AD is lipid dysfunction(3). The lipid bilayer of the Blood-Brain Barrier (BBB) endothelial cells harbors lipid rafts that play a vital role in transcytosis and maintaining various signaling functions(3). Lipid metabolism at the BBB changes with age and diet and results in a decrease of unsaturated fatty acid content and an increase in lipid peroxidation.

In this study, we hypothesize that the delivery of lipid nanoemulsion, which is rich in unsaturated fatty acids, will improve insulin signaling at the BBB, and ameliorate insulin resistance caused by cytokines like TNF- α . This, in turn, is expected to decrease VCAM-1 expression and mitigate BBB dysfunction. This hypothesis has been verified by treating BBB endothelial cells with inflammatory cytokines like TNF- α , which inhibited insulin signaling and increase the expression of vascular cell adhesion molecule-1 (VCAM-1), a marker for endothelial inflammation. Alternatively, exposure to soybean oil nanoemulsion (SNEs) like that of Humulin® triggered insulin signaling and reduced VCAM-1 expression. The results showed that the SNEs have the ability to overcome the resistance induced by TNF- α and increased the insulin signaling to the level comparable to Humulin® control and the opposite effect was seen when the cells were treated with nanoemulsion rich in saturated fatty acids. Lipid-based nanoemulsion could be

used as a strategy to mitigate insulin resistance and the consequent inflammation commonly seen in neurodegenerative disorders like AD.

Keywords: Lipid nanoemulsion, soybean oil, coconut oil, insulin resistance, inflammation, VCAM-1, insulin signaling

1.0 Introduction:

1.1 Alzheimer's Disease:

1.1.1 Alzheimer's Disease and Dementia:

Alzheimer's Disease (AD) is a progressive neurodegenerative disorder and has been identified as a leading cause of dementia. AD is thought to develop 20 years or more before the symptoms develop(4). The disease starts with changes in the brain that initially goes unnoticed and as the disease progresses the patient develops severe memory impairment and loses their ability to function independently. The current medications and treatments help to mitigate the symptoms of the disease and slow down the disease progression(5). However, most of these medications do not address core AD pathology.

As of 2021 just in the United States of America, more than 6 million Americans are living with AD and by 2050 this number is expected to double. During the COVID-19 pandemic, in the United States, AD-related deaths have increased by 16% and approximately 1 in 3 seniors die due to AD(4). This indicates that the disease kills more patients than breast and prostate cancer combined. Apart from the grave impact on the population, AD has a huge national cost. In 2021 it was estimated that AD and other dementia can cost the United States, approximately \$355 billion and by 2050, these staggering costs are estimated to increase to \$1.1 trillion(4). Globally it is estimated that close to 44 million people live with AD or a related form of dementia and has a global cost of \$605 billion, a figure which is estimated to double by 2050(4).

Although Alzheimer's disease etiology is not well understood, the disease has significant genetic and non-genetic risk factors, which play a role in disease development and progression(6). One of the main hallmarks of AD seems to be the build-up of amyloid-beta ($A\beta$) peptides in the brain. As the disease progresses, the amyloid plaques in the brain parenchyma and cerebral vasculature expands

into the cortex(7). A β peptides are generated from two consecutive cleavages of the amyloid precursor protein. One end of the APP peptide is formed by β -secretase's proteolytic activity, whereas the other end is formed by γ -secretase's proteolytic activity. These cleavage events form two main types of A β isoforms: A β 40 and A β 42(7). A β has the potential to cause neurotoxicity through inflammation or by boosting the free radical generation. The buildup of neurofibrillary tangles in neurons is the second distinguishing hallmark of AD. Tau protein, which is involved in microtubule formation, is abnormally folded and phosphorylated, resulting in tangles. The extent of tau tangles formation was found to correlate with the severity of the disease(7). Although, A β and tau proteins are typically implicated as the primary cause of AD-related synaptic loss and neuronal loss, AD pathology involves numerous additional components which contribute to the progression of the disease. These include cerebrovascular amyloidosis, degeneration of white matter, advanced age, diabetes, and lifestyle influences like Obesity. It has also been noted that AD demonstrates sex-dependent developmental and physiological differences. The disease disproportionately affects women, who make up two-thirds of AD patients. Even though recent studies indicate that incidents of AD appear to be similar in men and women, women appear to have a higher incidence of AD. In general, women progress more rapidly from mild cognitive impairment to severe cognitive decline(8).

Apart from gender differences, AD has a significant genetic risk component. Nearly 20 distinct genes have been linked to the likelihood of developing Alzheimer's disease(9). The ϵ 4 allele of the apolipoprotein E gene is the most significant risk factor for late-onset AD. APOE4 was found to increase AD risk in women more than in men. Other genetic factors such as APP, PSEN1, and PSEN2 mutations are seen in the early onset of familial AD. These 4 genetic risk factors make up 30-50% of inherited AD(9).

As of now, there are no interventions that can address the core AD pathology, most of the approved medications and treatment options show promising results in mitigating the disease. The recently approved drug Aduhelm targets the

fundamental pathophysiology of the disease. It was observed that a patient in the Aduhelm treatment group experienced a reduction of amyloid plaque burden, and this effect was determined to be time and concentration-dependent(10).

A combination of approved medications like Aduhelm and improved management of diseases that increase AD risk like obesity, hypertension, and diabetes will make it possible to control the progression of AD.

1.1.2 Stages of Alzheimer's Disease:

Alzheimer's Disease typically progresses slowly in 3 stages: early, middle and late AD. As mentioned earlier AD can start developing years before the onset of the disease, the stage where the brain undergoes pathological changes but without any clinical manifestation of the disease is regarded as the preclinical stage, in the early stage of the disease the patient can function independently. Common AD symptoms are not widely apparent at this stage, but the patient starts to lose their cognitive abilities, these symptoms worsen as the disease progresses to the later stages(11). By the late or the severe stage of the disease, a person cannot function independently and becomes completely dependent on a caretaker.

1.2 Blood-Brain Barrier:

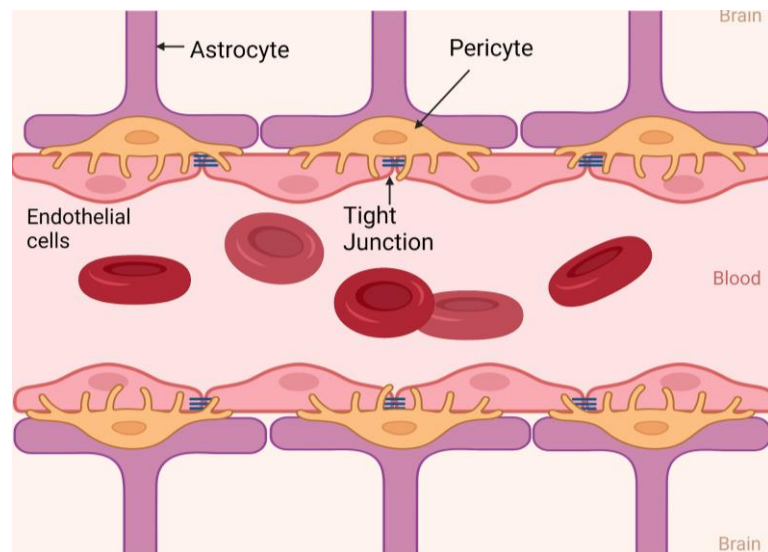
1.2.1 Blood-Brain Barrier- structure, function, and role in AD:

The Blood-Brain Barrier (BBB) is a highly selective barrier that exercises extensive control over the transport of the substances circulating in the blood. It has been proposed that the combined surface area of the barrier constitutes the largest interface for blood-brain exchange. The BBB endothelial cells differ from the endothelial cells by the absence of fenestrations, more extensive tight junctions which limits the paracellular flux of hydrophilic molecules across the BBB, and limited vesicular transport(12). Even though the barrier is selective it allows rapid exchange of oxygen and carbon dioxide from the blood to the brain, which is essential for normal brain metabolism and pH regulation in the interstitial fluid,

neurons, and other cells. Besides the gas exchange, the barrier also allows small lipophilic molecules with an average molecular weight of <400 Da and less than eight hydrogen bonds to cross without any hindrance(13). Essential molecules such as glucose, amino acids, and nutrients cross the barrier via receptor-mediated transport; larger molecules like iron transferrin and insulin can cross the barrier via receptor-mediated endocytosis(12).

Endothelial Cells:

One of the unique anatomical features of the neuronal system is the blood-brain barrier (BBB), it is made up of a monolayer of endothelial cells with tightly sealed cell to cell contacts(14). The endothelial cells are critical in terms of maintaining the properties of the blood-brain barrier(14). The CNS endothelial cells are held together by tight junctions, which control the movement of ions and molecules across the barrier. The endothelial cells have a low rate of transcytosis as compared to the peripheral endothelial cells and as a result, they greatly restrict the vesicle-mediated transport of solutes(14).



Created with BioRender.com

Fig 1: Schematic representation of Blood-Brain Barrier

Tight Junctions (TJs):

Brain endothelial TJs are key features of the BBB and are composed of integral membrane proteins: occludins, claudin junctional adhesion molecules (JAMs), and several cytoplasmic proteins like zonula occludens-1, -2, -3, etc. Adherens junctions are composed of cadherin-catenin complex and its associated proteins. This tight paracellular and transcellular boundary results in a polarized cell with distinct luminal and abluminal membrane compartments, allowing for precise regulation of blood-brain movement through specific cellular transport processes(12, 14).

Mural cells:

The microvasculature is incompletely covered by the mural cells. It includes pericytes which are found on the abluminal surface. These cells do not have any specific markers which is why they are often confused with other cells present on the abluminal surface. Pericytes are composed of contractile proteins and span over several ECs and control the diameter of the blood vessel(14). Through N-cadherin and connexins, they share a basement membrane with endothelial cells. Their relative proximity to endothelial cells allows for the exchange of ions, metabolites, other substances, etc. Angiogenesis, immune cell influx, and blood pressure modulation are all critical functions of pericytes. It has been reported that pericytes play a crucial role in the creation of BBB throughout development and the maintenance of BBB function as people age. The loss of Pericytes and formation of microaneurysm in PDGF-B deficient mice suggests that the pericytes play an important role in maintaining BBB integrity(15).

Astrocytes:

Astrocytes are star-shaped supportive glial cells that are abundantly found in the CNS. They are largely responsible for brain parenchyma compartmentalization, ionic homeostasis maintenance, pH management, neurotransmitter uptake, and signal mediation from neurons to endothelial cells. They express proteins called

Glial Fibrillary Acid Protein (GFAP). This protein aids astrocytes to form a link between neuronal circuits and blood vessels. This interaction helps the astrocytes to regulate the blood pressure in response to neuronal activity(14).

In humans, 4 types of astrocytes exist interlaminar, protoplasmic, varicose projection, and fibrous. Of these, protoplasmic astrocytes are the most commonly found. They are distributed throughout the grey matter of the cortical layer 1 thru 4(16). Due to the pervasive nature of these astrocytes, they are believed to play a role in modulating the blood flow. Astrocytes have long been thought to play a key role in CNS homeostasis, metabolic control, and neuroprotection. They also ensure the continued functioning of the neurons. Due to their broad scope of function, astrocytes have been considered as the target for various diseases.

Apart from maintaining homeostasis, the BBB protects neurons from factors present in the systemic circulation which have the potential to cause neuronal toxicity and thereby ensure neuronal health(17). The tight junction restricts the transport of ions and polar solutes across the membrane and limits the transportation of various macromolecules, some essential macromolecules like insulin can cross the barrier by receptor-mediated transcytosis or by a nonspecific mechanism. This unique anatomy of the BBB makes delivery across the barrier very challenging. To achieve efficient transport across the BBB, it becomes imperative to utilize its unique anatomical features.

As BBB is an important structure to maintain the brain homeostasis and for ensuring neuronal health, disruption of BBB results in the influx of various neurotoxic substances, cells, proteins, pathogens, etc. The BBB dysfunction has been regarded as an early biomarker for AD and plays a role in the initiation of inflammatory and immunological responses, which can set off the neurodegenerative cascade(17).

1.2.2 Blood-Brain Barrier dysfunction:

Patients suffering from various neurological disorders such as AD or Parkinson's disease (PD) often manifest BBB dysfunction. The BBB dysfunction, which results in decreased clearance of A β protein can in turn trigger an inflammatory response and eventually leads to neurodegeneration(18). Additionally, BBB dysfunction could be exacerbated due to the altered lipid profile in the endothelial lipid bilayer which results in altered membrane integrity and fluidity. The decline of cognitive function can be attributed to BBB dysfunction(19).

It is proposed has been proposed that Cerebral Amyloid Angiopathy (CAA) can contribute to AD pathogenesis by affecting the perivascular drainage which as a result affects the clearance of A β from the brain and it is one of the three pathological hallmarks for the disease(17). According to the two hits vascular hypothesis, damage to the blood vessels can trigger BBB dysfunction which as a result diminishes brain perfusion, this, in turn, leads to neuronal injury and accumulation of A β in the brain(20). The disruption to the BBB has the potential to be an independent cause or can act synergistically with A β to promote the progression of AD. This is further accelerated by genetic factors, hypertension, diabetes, dyslipidemia, etc(17).

The lipid raft integrity is another thing affected in the case of metabolic and neurodegenerative diseases such as AD. Lipid rafts are considered as dynamic structures that are majorly composed of cholesterol, sphingolipid, unsaturated lipids, phospholipids, etc. They have been known to play an important role in enhancing the protein-lipid, protein-protein interaction, and cellular signaling events(3). The presence of lipid rafts in the bilayer has been reported to improve the membrane integrity and fluidity of the endothelial cells. Lipid rafts also play an important role when it comes to the insulin and IGFR signaling necessary to maintain the metabolic and mitogenic function of the BBB(21).

In addition to lipid rafts, the BBB cell membrane is also enriched with various polyunsaturated fatty acids including DHA, EPA, ALA, etc. It has been determined that the unsaturated lipids found in membrane phospholipids play a critical role in maintaining cell integrity and cell membrane function. They are also involved in cellular signaling, energy balance, and inflammation(19).

Lipid metabolism at the BBB can change with age, which is noted by the decline in unsaturated fatty acid and increase in lipid peroxidation. Age-dependent lipidome changes at the BBB are one of the contributing factors to BBB disruption and accelerate the development of neurodegenerative disorders like AD(19).

1.2.3 Role of lipid dysfunction in AD:

Dietary lipids have an influence on both physiological lipid metabolism and the risk of developing Alzheimer's Disease. DHA and AA are mostly obtained from dietary intake of its shorter chained, less saturated counterparts, ALA and LA, respectively(19).

After consumption the fatty acid is anabolized in the body, thus creating the long-chain fatty acids. Before the modernization of human civilization, our diets were enriched with an equal balance of n-6/n-3 essential fatty acid(19)(22). Today's western diet has shifted our diet to an n-3/n-6 ratio of 1:17(19), meaning that a majority of the population has a diet rich in LA, AA, and DPA, which as a result produces inflammatory and oxidation mediators. This significant shift from an equal balanced diet to a diet rich in n-6 fatty acids has been associated with an increase in cognitive decline and AD(19).

Even though the human brains are high in long-chain omega-3 and omega-6 fatty acids, the significance of these fatty acids in numerous signaling pathways remains elusive(19). Lipidomic studies looking into AD pathology have demonstrated that a decrease in omega-3-fatty acid levels in the brain, predominantly in the hippocampus(23). This reduction of fatty acid in the hippocampus can be casually

correlated to impaired learning and memory abilities, thereby contributing to the onset of AD(24).

In addition to composing the BBB lipid bilayer, lipids in conjugation with various components of the lipid rafts are involved in receptor-mediated transcytosis within the CNS. These transport vesicles are essential for transporting the essential macromolecule across the BBB. A disruption in the lipid composition thereby can consequently affect the transport of these molecules across the BBB(25).

The role of DHA in this aspect has been widely studied. The fatty acid can disrupt the membrane domains such as caveolin-1 via controlling the expression of MFSD2A(26). This kind of control is essential for maintaining BBB integrity and suppresses transcytosis. A leaky barrier makes the brain more vulnerable to toxins and infections, disrupts homeostasis, and may lead to neuronal dysfunction(19). The level of fatty acid in distinct parts of the brain could be a viable biomarker to potentially identify the onset of Alzheimer's Disease, based on emerging evidence that the disease is linked to the disruption of fatty acid metabolism.

1.3 Insulin resistance and Inflammation:

1.3.1 Insulin Resistance:

A growing body of research implies a link between type 2 diabetes (T2D) and Alzheimer's Disease (AD). Various experimental observations have also identified the presence of markers of metabolic dysregulation in AD, most notable being insulin resistance. The exact molecular mechanism supporting this correlation remains to be identified.

The brain is an insulin-sensitive organ and requires it for various critical functions. Insulin can modify neuronal activity in the brain by promoting synaptic plasticity, it can improve memory function, the Insulin Receptor (IR) and Insulin-like Growth Factor Receptor 1 and 2 (IGFR) play an instrumental role in maintaining various

critical signaling pathways in the brain, additionally, insulin can also modulate pro-inflammatory function.

Studies have shown that insulin signaling is impaired in the brains of an AD patient and the experimental models(27). Diabetic insulin resistance and diet that promotes insulin resistance have been known to promote the risk of developing dementia. Studies have determined that T2D significantly increases the risk of dementia by 5 fold and diabetic insulin resistance could be one of the contributing factors(1).

Patients with insulin resistance, obesity, T2D, and low-grade chronic inflammation have higher circulating levels of pro-inflammatory cytokines such IL-6 and TNF- α (28). Increased inflammatory cytokines can inhibit insulin signaling by impairing tyrosine kinase activity of IR and Insulin Receptor Substrate (IRS)-1. It was found that mice that lacked TNF- α receptors were resistant to obesity-induced insulin resistance(29). Insulin resistance and compensatory hyperinsulinemia could be causally associated with elevated inflammatory markers(30).

It has been noted that hyperinsulinemia and inflammation have a bidirectional relationship. Hyperinsulinemia contributes to vascular inflammation, the inflammation leads to insulin resistance by impairing IR and IRS-1, which as a result causes a compensatory increase in circulating insulin(30).

Emerging evidence suggests that impaired BBB integrity plays a pivotal role in the onset and progression of neurodegeneration and cognitive impairment. Under normal circumstances insulin binds to IR which triggers the phosphorylation of the IRS-1, this results in the activation of the Pi3k/AKT pathway and downstream cellular response, which facilitates neuronal growth, neuronal survival, memory, learning, etc(31).

In Alzheimer's Disease, A β oligomers build-up, causing an increase in TNF- α and the activation of stress kinases including c-Jun N-terminal kinase (JNK), which leads to increased inhibitory serine/threonine phosphorylation of IR and a decrease

in insulin and insulin-like growth factor receptor expression. Insulin resistance lowers the expression of the A β -degrading insulin-degrading enzyme (IDE)(31).

The reduction of brain insulin signaling results in the reduction of AKT phosphorylation. This cascade pathway is of interest as phosphorylation of AKT governs the expression of GSK-3 β . And it has been speculated that an increase in GSK-3 β increases abnormal tau phosphorylation(31).

1.3.2 Inflammation:

Even though AD is considered to be a neurodegenerative, disease, vascular factors and BBB dysfunction could contribute to the progression of the disease. Cell Adhesion Molecules (CAM) such as Vascular Cell Adhesion Molecule-1 (VCAM-1) and Intercellular Cell Adhesion Molecule-1 (ICAM-1) might be activated as a result of endothelial/ BBB dysfunction. Studies have shown VCAM-1, ICAM-1, and E-selectin levels were elevated in AD patients(32). Additionally, as compared to other cellular adhesion molecules, increased levels of VCAM-1 levels have been linked to advanced dementia stages, significant E-selectin levels were found in patients with mild dementia stages (33).

VCAM-1 and ICAM-1 both belong to the immunoglobulin superfamily, but VCAM-1 is exclusively present on the endothelial cells and ICAM-1 was found on leukocytes, astrocytes, and within senile plaques. VCAM-1 has emerged as the biomarker to detect endothelial dysfunction since the adhesion molecule is specifically found on the endothelial cells(34).

In addition to the severity of dementia, other factors such as aging, hyperhomocysteinemia, and lipid profile could affect the levels of VCAM-1.

Clinical studies have shown that patients experiencing early dementia stages, showed cognitive and memory improvement when they had a diet rich in omega-3 fatty acids, such as Docosahexaenoic Acid (DHA), Eicosapentaenoic acid (EPA),

and α -Linolenic Acid (ALA), however, which fatty acid plays a primary role in mitigating dementia symptoms is still debated(35, 36).

Omega-3-fatty acids could have an influence in improving dementia symptoms as they are an important component of the cell membrane. Omega-3-fatty acid could also be beneficial in the case of AD due to its antioxidant, anti-inflammatory, antiapoptotic and neurotrophic properties(37).

Additionally, various animal models have shown that the ratio of omega-3-fatty acid and omega-6-fatty acid exerts an influence on various serotonergic and catecholaminergic neurotransmissions, which are affected first during AD. When Phospholipase A2 (PLA2) (an enzyme that cleaves fatty acid) hydrolyzes the membrane fatty acid, it liberates omega-6-fatty acids, which are then metabolized to prostaglandins. Prostaglandins generated by omega-6-fatty acid metabolism have a higher inflammatory potential as compared to those generated by omega-3-fatty acid. PLA2 activity combined with an altered lipid profile could play a role in the progression of AD.

Studies have shown that omega-3-fatty acids can mitigate the TNF- α induced expression of VCAM-1(38) Additionally there have also been studies that report that the omega-3- Fatty acid also has an inhibitory effect on IL-1 β .

1.4 Delivery across the BBB:

1.4.1 Nanoparticles:

The BBB plays a significant role in maintaining homeostasis and protecting the CNS; however, the effective barrier property of the BBB becomes a hindrance when it comes to delivering therapeutics to the CNS. Typically a small lipophilic molecule with a molecular weight <400 Da can cross the BBB effectively and as a result, most macromolecules cannot cross the barrier. To overcome this limitation, nanocarriers have been extensively used. Nanocarriers can be modified to achieve the desired drug payload, delivery rate, and effect of the therapeutics(13) and as a result, these

carriers have been used to deliver not only therapeutics but also diagnostic markers across the BBB.

Typically a nanoparticle with a size <200 nm can penetrate leaky tumor tissue, however for delivery into the brain, a smaller nanoparticle size does not necessarily mean enhanced delivery(39) for instance a PEG-PLA protein complex nanoparticle cannot cross the healthy BBB, however, the nanoparticle can effectively deliver a brain-derived neurotrophic factor (BDNF) in a middle cerebral artery occlusion mouse model for stroke. The nanoparticle can effectively cross the BBB due to the disruption caused by the stroke(39).

1.4.2 Nanoemulsion:

Nanoemulsions (NEs) are one of the popular colloidal formulation systems in the pharmaceutical industry. Nanoemulsions have a size ranging from 10 to 1000 nm(40) which confers high thermodynamic and kinetic stability and as a result, they are being rapidly used as a system of drug delivery(41).

Nanoemulsions can be classified based on their morphology. An oil in water emulsion has oil dispersed in a continuous water phase (o/w) whereas an inverse of this is called water in oil phase(41). The two immiscible phases are typically stabilized with the help of surfactants. During the emulsification process, the surfactants minimize the coalescence by absorbing the oil and water interphase(40), thereby lowering the surface tension. The surfactants also aid in the dispersion of the oil in o/w emulsion by forming an interfacial film.

The potential of the NEs for improving the quality and efficacy of the medicinal compounds has been demonstrated in various medical formulations. The larger surface is to volume ratio of NEs enhances the absorption and efficacy of the encapsulated drug.

Encapsulating the drug within the NEs protects the active ingredient from environmental, pH changes as well as enzymatic degradation(40). This particular

property has been handy when it comes to beating the COVID-19 pandemic. It protects the antigen from premature degradation, which ensures an enhanced immune response, reduces adverse events, and facilitates intracellular uptake(42).

1.4.3 Formulation of nanoemulsion:

Nanoemulsions mainly have 3 major components 1) the lipid core 2) surfactants 3) the fluorescent or the therapeutic molecules. The emulsions can be formulated using various techniques:

1. Phase inversion technique: This method does not necessitate the use of an external force. It involves the creation of fine dispersion as a result of temperature changes or composition while keeping the other parameters constant during phase transition(43).
2. Brute force method: This approach utilizes force for breaking the oil droplets into the nanometer range, this includes the use of a high-pressure homogenizer, high-speed mixer, small pore membrane, etc. In this method, the properties of nanoemulsion such as size and stability depend on multiple variables like the degree of mixing, emulsification time, etc(43).
3. Spontaneous emulsification: The emulsion is prepared in three stages: the first is the development of the organic phase, which consists of the oil and a lipophilic surfactant in a water-miscible solvent, and the second is the formation of the hydrophilic surfactant. The o/w emulsion is made by infusing the organic phase into the aqueous phase while stirring it under a magnetic stirrer. Evaporation is used to remove the organic solvent(43).

In our study, the main lipid core comprised of soybean oil, coconut oil, and fish oil. These oils have different concentrations of unsaturated/saturated fatty acids and served as the source for determining the effect of unsaturated and saturated fatty acids on the BBB.

DOTAP (1,2-dioleoyl-3-trimethylammonium-propane as a chloride salt) and DPPC (1,2-dipalmitoyl-sn-glycero-3-phosphocholine) were used as the surfactants in the

ratio of 3:2, which was kept constant through all formulations. DOTAP has a net positive charge and DPPC is a zwitterion.

DOTAP's net positive charge enables the positively charged nanoparticle to effectively interact with the negatively charged cell membrane, thus ensuring an effective uptake of the nanoemulsion, in addition to this the surfactants makes the formulation stable and minimize the chances of creaming. DPPC has a phospholipid functional group, which is also the main component of the cellular membrane. The amphiphilic functional group makes DPPC biocompatible. DPPC has widely used for pharmaceutical formulations such as nanoemulsion as it not only confers stability but helps achieve sustained release of a drug(44). Emulsions containing DPPC as demonstrated reduced spleen distribution and as a result, the emulsion can have a prolonged plasma circulation(44).

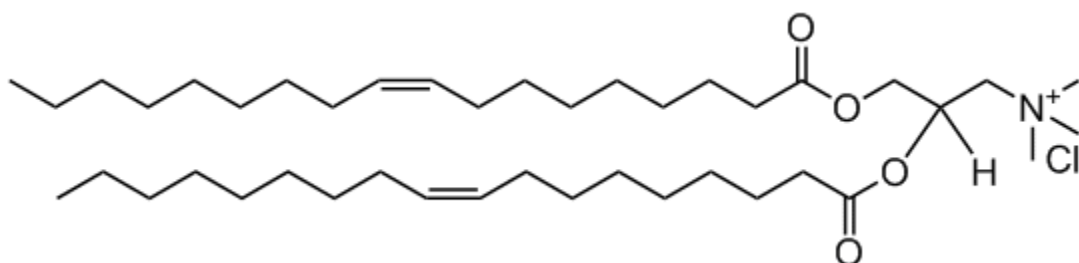


Fig 2: Structure of 1,2-dioleoyl-3-trimethylammonium-propane (DOTAP) as a chloride salt

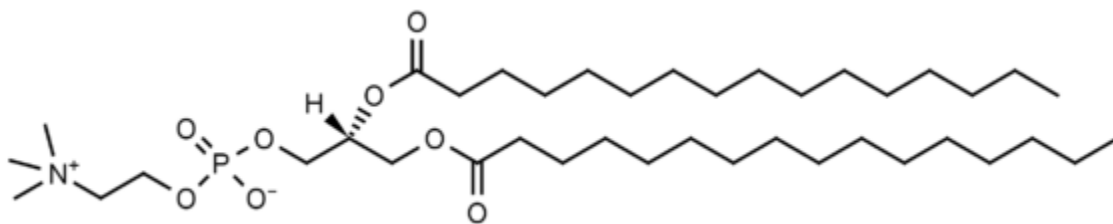
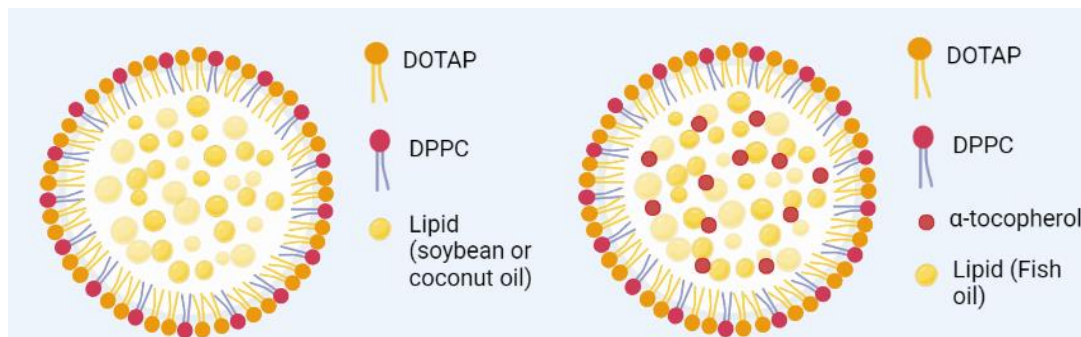


Fig 3: Structure of 1,2-dipalmitoyl-sn-glycero-3-phosphocholine (DPPC)

Additionally, we used the fluorescent compound, 1,1'-dioctadecyl-3,3,3',3'-tetramethyl indocarbocyanine (Dil-C18) as a fluorescent marker for the lipid component.



Created with BioRender.com

Fig 4: Schematic representation of lipid nanoemulsions.

As described briefly above, nanoemulsion can be formulated using a high or low energy method. High energy methods typically employ the use of mechanical force such as ultrasonic waves, high-pressure homogenizers, etc to obtain the ideal particle size. On the other hand, the low energy method relies on the principle of spontaneous emulsification or emulsion phase inversion (EPI) for the formulation of the nanoemulsion.

Lipids with long-chain triglycerides can form larger oil droplets due to their lipid phase viscosity(45), therefore we utilized a high-energy method to formulate our nanoemulsions to obtain the desired particle size.

Characterization of nanoemulsion:

1. Particle size determination: The particle size of the NEs is typically analyzed with the help of light scattering because of the Brownian motion of particles as a function of time. It is based on the idea that a particle with a smaller size travels at a faster rate than a particle with a larger size(43).
2. Zeta potential: Zeta potential is used for measuring the surface charge of the particle when dispersed in a liquid. Zeta potential gives us an estimate of the

dispersion stability and the zeta value depends on the physicochemical property of drug, polymer, vehicle, presence of an electrolyte, etc(43). Malvern zeta sizer is typically used for measuring the zeta potential. Higher zeta-potential would mean highly charged particles, which would as a result minimize the potential of aggregation due to charge repulsion. If the zeta potential is low, the attraction will overcome repulsion and the particles will aggregate. A Zeta potential of ± 30 mV is thought to be sufficient for ensuring the nanoemulsion's physical stability(43).

1.5 Current treatments:

Current treatments of this disease include using cholinesterase inhibitors such as donepezil, rivastigmine for all stages of AD, and Memantine for moderate to severe cases. These interventions can improve the patient's standard of living to an extent other than that the medications do not affect the disease progression and rate of decline(46).

The FDA recently approved Aduhelm (aducanumab) a human immunoglobulin gamma 1 (IgG1) mAb to treat patients with Alzheimer's Disease under its accelerated approval program. The approval was a significant milestone as it is the first novel therapy to be approved for AD since 2003. Aduhelm is the first treatment directed towards the accumulated soluble and insoluble forms of A β , it reduces, thereby reducing the A β levels in the brain. The treatment is now approved for people with mild dementia(47).

Many studies have also implicated inflammation as one of the causative factors for AD progression, therefore there have been efforts to mitigate inflammation using Non-Steroidal Anti Inflammatory Drugs (NSAIDs), but the studies failed to show any significance. On a similar path, the use of omega-3- fatty acids has recently generated interest due to their cardiovascular benefits. Two recent randomized, controlled, double-blinded studies have demonstrated that fish oil supplements can improve thinking and memory in patients with Mild Cognitive Impairment(46).

Additionally, a preclinical study has also demonstrated omega-3-fatty acid-rich fish oil can counteract A β toxicity by promoting A β clearance by increasing the expression of LRP-1(48).

2.0 Statement of problem:

2.1 Statement of the problem:

We aim to address the BBB dysfunction-induced inflammation by administering a lipid formulation consisting of various oils such as fish oil, soybean oil, and coconut oil.

It has been previously established Wang et al that soybean nanoemulsion (SNEs) has the potential to upregulate insulin signaling. The study noted a 2 fold increase in AKT phosphorylation in the presence of insulin plus SNEs in comparison to control. No significant changes were noticed when hCMEC/D3 cells were treated with olive oil nanoemulsions (ONEs)(49).

According to the study published in the journal of Diabetologia by R.Madonna et al, in the state of hyperinsulinemia, insulin can potentiate VCAM-1 expression in human umbilical vein endothelial cells, according to study, insulin increased VCAM-1 expression in a concentration-dependent manner and this effect was even more significant in the presence of Pi3K inhibitor, which indicates that in the state of insulin resistance, VCAM-1 expression increased(50).

In another study that looked at VCAM-1 expression in the presence of TNF- α and Insulin, it is postulated by the author that the synergistic effect seen with TNF- α and insulin, could be due to TNF- α induced insulin resistance in human umbilical vein endothelial cells(51). This upregulation could be due to the activation of NF-kB.

When we look at the findings published by Ohkawa et al in the journal of pharmacy and pharmacology, it was observed that when male rats were given TPN without soybean fat for 4 days, the rats developed hyperglycemia, hyperinsulinemia, and

hypotriglyceridaemia. These disorders were mitigated when the rats were given TPN with soybean oil. The study also observed that rats who were given fat-free TPN also developed insulin resistance(52). Finally, based on the ongoing studies being conducted in our lab, which was presented in AAPS 2020, it was determined that A β -42 significantly upregulated VCAM-1 at BBB in comparison to A β -40. Additionally, the study also concludes that the SRC-FAK-MAPK pathway could be involved in the upregulation of VCAM-1 at the BBB(53).

For our study, we formulated nanoemulsions with different concentrations of saturated and unsaturated fatty acids.

The saturated fatty acid content of fish oil might range from 27.68% to 36.59%, monounsaturated fatty acids from 8.99% to 35.8%, and polyunsaturated fatty acids from 10.69% to 39.57%. Eicosapentaenoic acid (C20:5n-3) has a concentration of 1.72% to 10.73%, while docosahexaenoic acid (C22:6n-3) has a concentration of 4.07% to 31.44%(54).

Palmitic acid (16:0) 10%, stearic acid (18:0) 4%, oleic acid (18:1) 18%, linoleic acid (18:2) 55 %, and linolenic acid (18:3) 13% are the five fatty acids found in soybean oil(55).

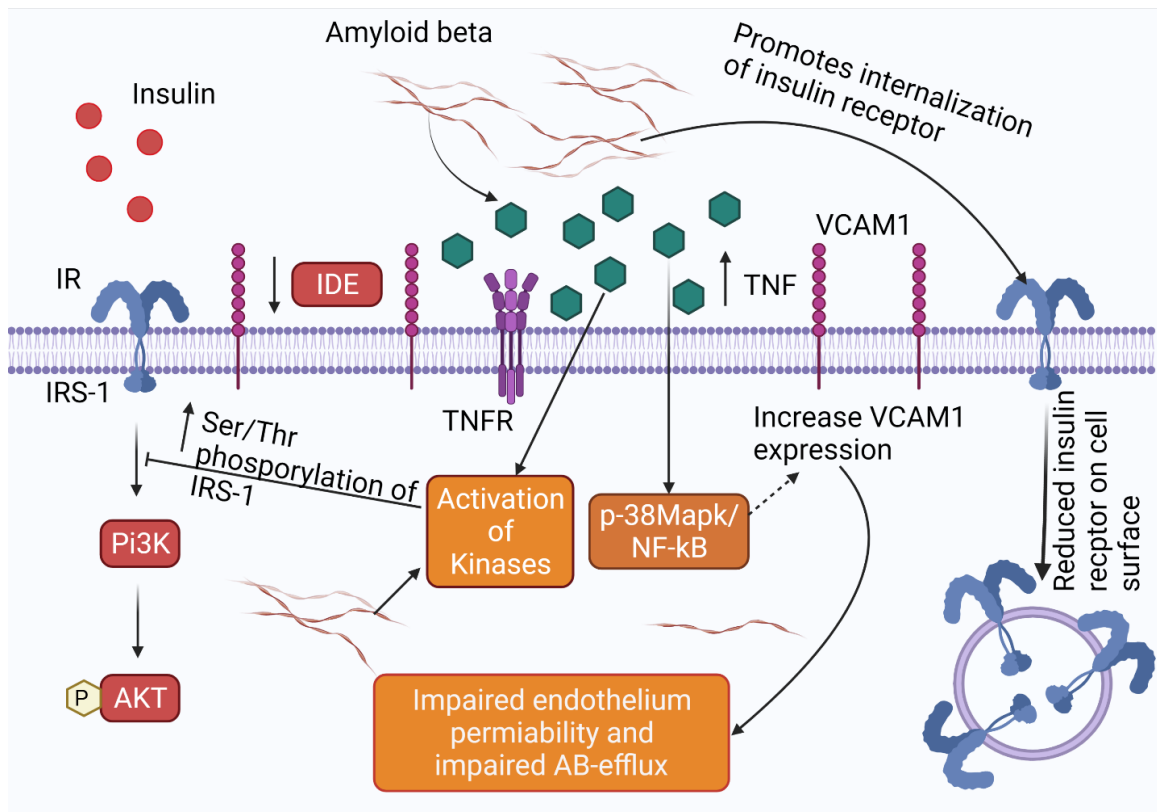
8% caprylic acid (8:0), 7% capric acid (10:0), 49% lauric acid (12:0), 8% myristic acid (14:0), 8% palmitic acid C (16:0), 2% stearic acid C (18:0), 6% oleic acid (18:1), and 2% linoleic acid (18:2) are among the fatty acids found in coconut oil (56) .

Oils	SFAs	MUFAs	PUFAs
Coconut oil	82%	6%	2%
Soybean oil	14%	18%	60%
Fish oil	27.61%	36.59%	35.8%

Table 1: Summary of fatty acids in Coconut, Soybean, and Fish oil

With these findings in mind, we decided to look into the effect of nanoemulsion on improving insulin signaling after the cells were exposed to TNF- α and A β -42.

We postulate as seen in **Fig 5**, that TNF- α activates the inflammatory process via the NF- κ B or the p-38MAPK and as a result, there is an upregulation of the inflammatory marker VCAM-1. A β oligomer further stimulates the release of TNF- α and as a result, there is a further potentiation of TNF- α action and since inflammation impairs ab efflux there is additional potentiation of the stress kinases, which according to Bedse et al results in inhibitory serine/threonine phosphorylation of the IRS-1. This inhibits the insulin the essential Pi3K/AKT signaling at the BBB. In addition to this, AB oligomer could further promote the internalization of IRS-1, thereby reducing the AKT signaling even further. (31)



Created with BioRender.com

Fig 5: Schematic representation of TNF- α mediated VCAM-1 expression and Pi3K pathway inhibition

We hypothesize that under the conditions where insulin signaling is downregulated (due to TNF- α or A β), the nanoemulsion containing unsaturated fatty acid would be able to overcome the resistance and as a result can also have an anti-inflammatory effect. We aim to establish this effect by observing the downregulation of VCAM-1 expression and upregulation of insulin signaling in the presence of TNF- α and A β -42 followed by the nanoparticle treatment.

2.2 Specific Aims:

Aim 1: Formulate and characterize nanoemulsions with different degrees of unsaturated fatty acids.

Aim 2: Establish the effect of TNF α and A β -42 on insulin signaling and compare the mitigating effect of the nanoemulsions.

Aim 3: Establish the inflammatory effect of TNF α and A β -42 and compare the mitigating effect of the nanoemulsions.

For formulating the nanoemulsions, DOTAP (1,2-dioleoyl-3-trimethylammonium-propane as a chloride salt) and DPPC (1,2-dipalmitoyl-sn-glycero-3-phosphocholine) were used as the surfactants in the ratio of 3:2 w/w, which was kept constant through all formulations. For encapsulating soybean oil, coconut oil, and crude fish oil with a fluorescent dye, Dil-C18. Soybean oil contains more polyunsaturated fatty acids (PUFA) compared to coconut oil which has more saturated fatty acids (SFA). Fish oil contains more omega-3 fatty acids such as DHA and triglycerides, this makes this oil very prone to oxidation. We utilized a crude source of fish oil, which could be used for our experimental purposes. The crude source had close to 30% of stearic and palmitic acid and close to 25% of omega-3 fatty acids and triglycerides and we incorporated 0.25% α -tocopherol to minimize any oxidation. The nanoparticles were subjected to particle size reduction using the pores of a single clean, track-etched polycarbonate membrane (50 nm, 100 nm). The formulation and particle size reduction were done under minimum light. The nanoparticle size was determined by Nanoparticle Tracking Analyzer (NTA) and

Dynamic Light Scattering (DLS). The cells were grown as a monolayer on 6 well plates for western blot analysis, this was used to investigate the impact of TNF α , A β -42, and nanoemulsion on p-AKT/AKT expression (which is the primary downstream marker in the insulin signaling pathway) Additionally, the cells were grown on confocal dishes to determine the effect of the nanoemulsion on VCAM-1 expression.

3.0 Material and methods:

3.1 Nanoemulsion formulation and characterization:

3.1.1 Materials:

The nanoemulsions were formulated using 1,2-dioleoyl-3-trimethylammonium-propane as chloride salt (DOTAP) and 1,2-dipalmitoyl-sn-glycero-3-phosphocholine (DPPC) were purchased from Avanti Polar Lipids, Inc. (Alabaster, AL). Soybean oil, coconut oil, and fish oil were purchased from Sigma-Aldrich (St. Louis, MO). The fluorescent compound, 1, 1'-dioctadecyl-3, 3', 3''-tetramethyl indocarbocyanine (DiI-C18), was purchased from Frontier Chemical (Boulder, CO). The human basic fibroblast growth factor (bFGF) was purchased from PeproTech (Rocky Hill, USA). Fetal bovine serum (FBS) was purchased from Atlanta Biologics (Flowery Branch, GA). Dulbecco's phosphate-buffered saline (DPBS, 1X) was purchased by Mediatech (Manassas, VA). All other chemicals were of analytical grade.

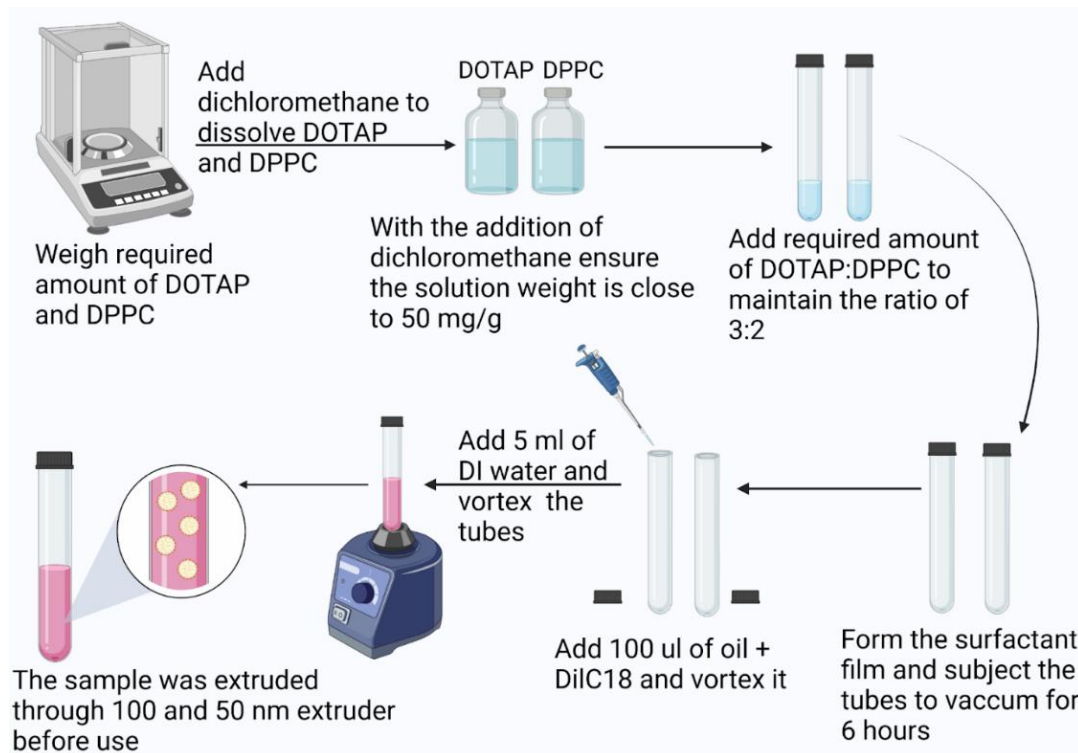
3.1.2 Nanoemulsion formulation:

The lipid nanoemulsion was prepared using the method established in our lab(49). The lipid nanoemulsions dispersed in distilled water were prepared on a weight basis. A stock solution of the surfactant was prepared using dichloromethane and the concentration was maintained at 50mg/g. DOTAP and DPPC were mixed in a 3:2 w/w ratio from the stock solution in pre-weighed Pyrex screw cap test tubes. The

ratio of the surfactants was kept constant for all formulations and was used to encapsulate soybean, coconut, and fish oil.

The surfactants were then dried as a thin film under nitrogen gas in a fume hood. The surfactant film was dried under vacuum (Edwards High Vacuum Int. Part of BOC Ltd. Crawley, Sussex, England) for 6 hours to eliminate any remaining solvent. The dry weight of the test tubes was recorded.

The surfactant film was then rehydrated using 1 mg/mL solution of DiIc18 in oil (100 μ l) and was vortexed to ensure uniformity. Further, 5 ml of distilled water was added and after recording the final weight the sample was vortexed until a uniform dispersion was obtained. The samples were then stored at 4 °C overnight.



Created with BioRender.com

Fig 6: Diagrammatic representation of formulating soybean oil (SNEs) and coconut oil (CNEs) nanoemulsions

Prior to use, approximately 0.6 ml of the NEs were drawn into 1 ml syringes and was subjected to size reduction using a clean track-etched polycarbonate membrane (pore sizes 50 nm, 100 nm) (NanoSizer™ Mini Extruder; T&T Scientific Corporation, Knoxville, TN) positioned in a small-volume extruder. The extrusion was carried out at ~50 °C by passing through the extruder 21 times through a 100 nm membrane followed by a 50 nm membrane.

A similar protocol was followed while formulating fish oil nanoemulsion (FNEs). We also incorporated 0.25 % v/v α -tocopherol into the crude fish oil to minimize oxidation and the final 5 ml emulsion was sealed under nitrogen and stored at 4°C for further experiments.

3.1.3 Nanoemulsion characterization:

The mean hydrodynamic diameter of the nanoemulsion dispersed in distilled water was determined using the NanoSight LM-10 model (Malvern Instruments Ltd., Malvern, UK). The movement of the particles was tracked using the Brownian motion of the individual particles which were recorded by the sCMOS camera at 30 frames/second. The video of the moving particles was captured and analyzed as 5 replicates by the nanoparticle tracking 2.3 image analysis software (NanoSight, USA) to assess the displacement of the particle in the x-y plane (**Fig 7: image B and C**). The displacement of the particle was then used to estimate the diffusion coefficient, using which the hydrodynamic diameter was calculated using the Stokes-Einstein equation. The mean, median, and distribution standard deviation values were determined for each sample and generated by the software. The mean and standard deviation of the number particles per mL were also determined.

Zeta potential (surface charge) was determined with the help of dynamic light scattering (DLS) using Malvern Zeta Sizer with folded capillary zeta cell. The aqueous NEs were further diluted in distilled water before analysis. The temperature for analysis was maintained at 25°C. The mode \pm standard deviation

was used for reporting particle size analysis and mean \pm standard deviation was used for reporting the zeta potential.

3.2 Cell culture:

The BBB model was created in vitro using human cerebral microvascular endothelial cells (hCMEC/D3 cell line was a kind gift from P-O. Couraud (Institut Cochin, France)). The cells were grown in an endothelial cell basal medium at 37°C and 5% CO₂ (Sigma-Aldrich, St. Louis, MO), with 5% v/v FBS. The cells were cultured in endothelial cell basal media supplemented with 1% v/v FBS for 12 hours before the experiment.

3.3 Western blot:

The hCMEC/D3 cells were cultured on 6 well plates. The cells were grown in 5% D3 media and were switched to 1% D3 media \pm TNF- α (R&D systems, USA) 12 hours before the experiment. Based on the ongoing work in our lab, AB-42 peptide was used to determine the upregulation of VCAM-1 and was added to the 1% D3 media incubated cells for 15 mins. The cells were further treated with SNEs or CNEs for 1 hour and were further incubated with 100 nM AF-647 labeled insulin for 20 minutes.

After the insulin treatment, ice-cold Dulbecco's PBS was used to wash the cells. This was followed by the addition of 50 μ l of radio-immunoprecipitation assay (RIPA) buffer (Thermo Scientific, Waltham, MA) containing EDTA-free protease inhibitor cocktail (Roche, Branford, CT) and phosphatase (Roche, Branford, CT), The cells were dislodged from the 6-well plates using a cell scraper. The cell lysates were then centrifuged at 10,000 rpm for 10 min at 4 °C. The total protein content was evaluated using the bicinchoninic acid (BCA) assay (Pierce, Rockford, IL) on a 96-well plate and examined at 562 nm using a standard plate reader After determining the protein concentration, lysate samples for western blot were prepared using DPBS and loading buffer (reducing agent+ XT buffer). The samples were warmed \sim 80°C for 7 minutes and subjected to centrifugation at 1000 rpm for 1 minute.

The 10µg/20ml samples were loaded on Criterion™ XT Precast gel and Thermo Scientific™ PageRuler™ plus prestained protein ladder was used as the protein marker. The sample was run for 1.5 hours in Tris-Glycine buffer. The gel was then transferred to a nitrocellulose membrane (Bio-Rad Laboratories Inc., Germany) and was blocked using 5% milk protein for 1 hour. The membrane was then rinsed with TBST and incubated with 1:1000 p-AKT, GAPDH, VCAM-1, and Vinculin primary antibodies (Cell Signaling, New England BioLabs, Beverly, MA) overnight at 4°C.

After the overnight incubation, the membrane was incubated with 1:2000 horseradish peroxidase linked Anti-Rabbit IgG secondary antibody (Cell signaling technology) in 5% milk protein for 1 hour, after washing the membrane 3X with TBST and 1X with TBS, the membrane was imaged LI-COR and analyzed on Image Studio Lite version 5.2 and the densitometry data generated was further analyzed on GraphPad Prism 9 (La Jolla, CA).

3.4 Antibody and protocol optimization for confocal microscopy:

The hCMEC/D3 cells were cultured on 35 mm coverslip dishes. The cells were grown in 5% D3 media and were switched to 1% D3 media ± TNF-α 12 hours before the experiment. 3 dishes were treated with Ice cold 100% methanol for 10 minutes and the other 3 dishes were treated with 4% PFA for 10 minutes at RT followed by 0.1% Triton X-100 for 10 minutes at RT. A secondary alone treated confocal dish was used as the control and the dishes were treated with primary VCAM-1 from Abcam (EPR504, Abcam) and VCAM-1 P3C4 (Developmental Studies Hybridoma Bank, The University of Iowa, Iowa City, IA). The two antibodies with different permeabilization methods were compared.

3.5 Confocal microscopy:

The hCMEC/D3 cells were cultured on 35 mm coverslip dishes. The cells were grown in 5% D3 media and were switched to 1% D3 media ± TNF-α 12 hours before the experiment. AB-42 peptide was used to determine the upregulation of VCAM-1 and was added to the 1% D3 media incubated cells for 15 mins. The cells were

further treated with the nanoemulsion for 1 hour and were further incubated with 100 nm AF-647 labeled insulin for 20 minutes.

After completing the 12 hours of incubation with 1% D3 media, the cells were rinsed with 500 ul of cold 0.1% PBST (PBS+ Tween 20), followed by incubation with 4% PFA for 10 minutes at room temperature. After rinsing with cold PBS, the cells were perfused with 0.1% TritonX-100 for 10 minutes at room temperature. The cells were then incubated with 10% goat serum for 30 minutes to avoid nonspecific binding. The cells were washed with cold PBS and then incubated with 1:250 anti-VCAM-1 (EPR5047, ABCAM) antibody in 1% BSA for 1 hour at room temperature. After washing the cells with PBS the cells were finally incubated with 1:1000 AF-647 labeled goat anti-rabbit IgG secondary antibody (Cell Signaling Technology, Danvers, MA) in 1% BSA for 1 hour at room temperature in dark.

The dishes were kept overnight to dry in a dark place and the dishes were mounted using ProLong Diamond Mounting medium (Invitrogen, Carlsbad, CA), and was kept overnight before imaging the dishes using Zeiss LSM 780 laser confocal microscope equipped with a C-Apochromat 40x /1.2W objective. The images were then analyzed with the help of Zen 3.2 blue edition software.

3.6 Statistical Analysis:

GraphPad Prism was used to conduct all statistical tests (GraphPad Software, LA Jolla, CA). The statistical significance of the difference in phosphorylation of AKT of cells treated with/without nanoemulsion and the difference in fluorescence intensity of VCAM-1 expression was evaluated by one-way ANOVA followed by Tukey's post-test.

4.0 Results:

4.1 Preparation and characterization of the lipid nanoemulsions:

The lipid nanoemulsion was prepared using the method described above. The surfactants DOTAP and DPPC were insoluble in water, hence their solution was prepared in dichloromethane. The surfactant solution was then cast as a thin film at the bottom of the test tube with the help of nitrogen and then dispersed in a lipid phase conjugated with DiI C18. Before each experiment, 0.6 ml of the nanoemulsion was extruded through membrane filters with a pore size of 100 nm and 50 nm, in the manner described above.

A	Nanoemulsion (3:2 DOTAP:DPPC)	Particle size (nm)	Zeta potential (mV)
	Coconut oil	160.0 ±123.6	+59.2
	Soybean oil	177.4 ±138.8	+59.4
	Fish oil	187.5 ±143.0	+33.9

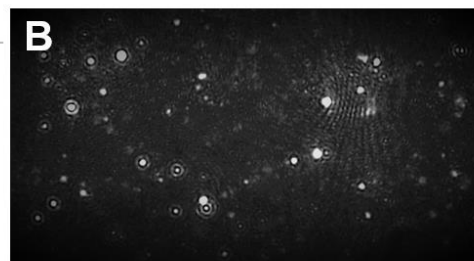


Fig 7: (A) Summary of particle characterization of various nanoemulsions **(B)** particle size analysis using NanoSight.

Characterization: Various parameters pertaining to the physical characterization of lipid nanoemulsions, including particle size and zeta potential are shown in **Fig 7 table A** and the representative image of particle size analysis from the nano tracker is depicted in **Fig 7: image B and C**. The mean hydrodynamic diameter of coconut oil nanoemulsion (CNEs) was 160.0 ±123.6 nm, 177.4 ±138.8 nm for soybean oil nanoemulsion (SNEs), and 187.5 ±143.0 nm for fish oil nanoemulsion (FNEs). The

mean zeta potential value for CNEs was +59.2 mV, for SNEs it was +59.4 mV and for FNEs it was +33.9 mV.

4.2 Effect of TNF- α on insulin resistance and inflammation in BBB endothelial cells:

4.2.1 Time-dependent effects of TNF- α exposure:

The hCMEC/D3 cells grown on 6-well plates were incubated with 1% FBS media with TNF- α (10ng/ml) for 6 and 12 hours followed by 20 minutes of 100nm Humulin® exposure and were compared to control cells treated with Humulin® alone. Time dependence of TNF- α exposure on insulin signaling was assessed by using various incubation times and the changes in p-AKT expression were determined using western blot analysis.

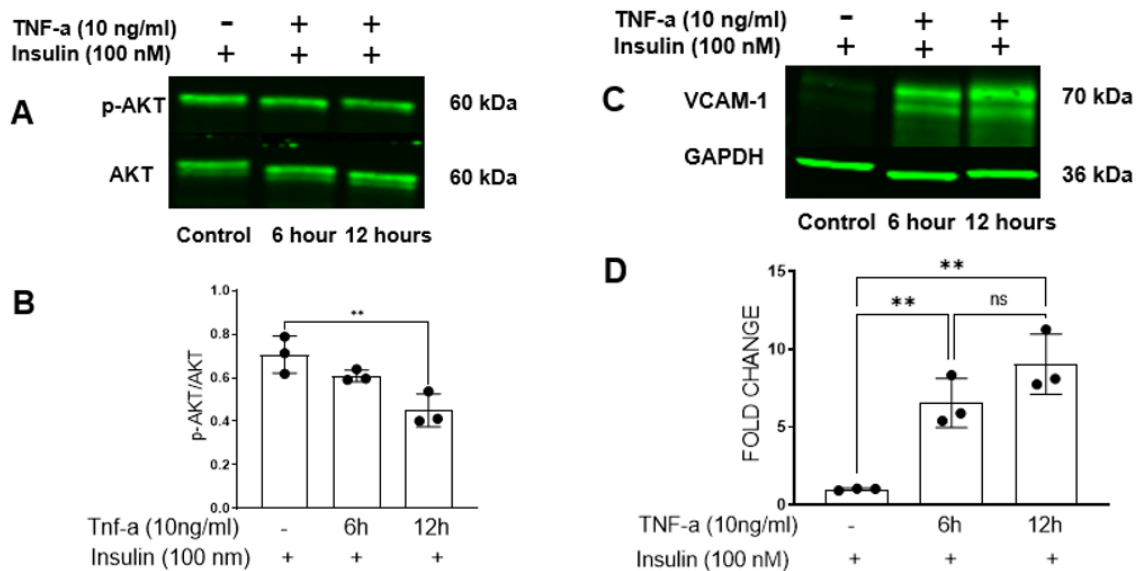


Fig 8: (A) Western blots showing the expression of p-AKT and AKT with and without TNF- α exposure. **(B)** Quantitation of p-AKT/AKT ratios **(C)** Western blots showing the time-dependent effect of TNF- α on VCAM-1 expression **(D)** Fold change in VCAM-1 expression with various treatments (One-way ANOVA with Tukey's post-tests, **p<0.01 and ***p<0.001)

We have identified that 12-hour incubation significantly reduced the p-AKT/AKT ratio in comparison to the control group (0 hours) **Fig 8: images A and B**. A similar trend was observed for VCAM-1, which demonstrated a 6 fold increase in VCAM-1 expression after 6 hours of incubation and a 9 fold increase in VCAM-1 expression after 12 hours of incubation with TNF- α as seen in **Fig 8: image C and D**. For further studies, the TNF- α exposure was set for 12 hours in 1% FBS.

4.2.2 Antibody and protocol optimization for confocal microscopy:

Confocal dishes were treated with 1:250 VCAM-1 Abcam antibody with methanol permeabilization and 4% PFA + 0.1% Triton X-100 permeabilization and 1:250 VCAM-1 P3C4, from Developmental Studies Hybridoma Bank antibody with methanol permeabilization and 4% PFA + 0.1% Triton X-100 permeabilization were compared. Methanol is commonly used as both permeabilization and fixation agent which is why it was not used in combination with 4% PFA (another commonly used fixation agent). we decided to compare methanol's permeabilization potential with Triton X-100 to determine the optimal permeabilization and fixation method for future confocal experiments.

Based on what was observed in **Fig 9: images B, C, E, and F** It was determined that in comparison to control and cells treated with P3C4, the dishes treated with Primary VCAM-1 Ab from Abcam had better signal. In comparison between the two permeabilization methods, it was determined that cells treated with Abcam antibody with 4% PFA+ 0.1% TritonX-100 showed a stronger fluorescent signal in comparison to methanol permeabilized cells. Therefore for the rest of the confocal experiment, VCAM-1 antibody from Abcam was used as the primary antibody and 4% PFA+ 0.1% Triton X 100 was used as the permeabilization method.

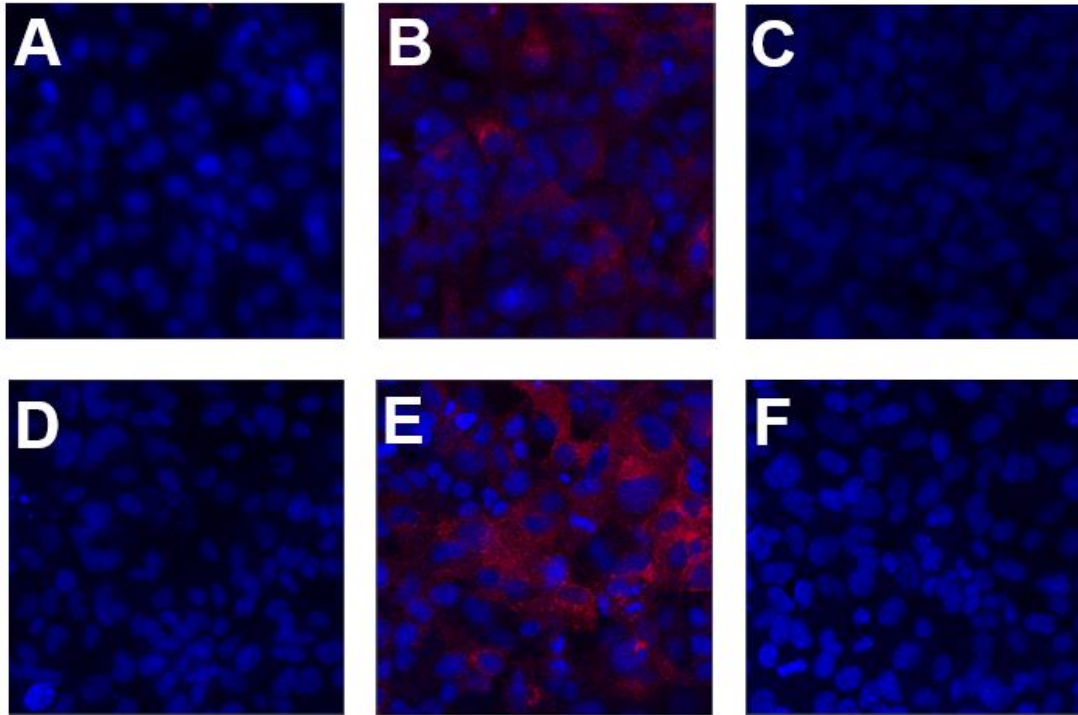


Fig 9: Confocal images of VCAM-1 expression detected by immunocytochemistry using two different primary antibodies and permeabilization methods. **(A)** Cells incubated with 1:1000 AF-647 labeled goat anti-rabbit IgG (secondary antibody) and permeabilized with methanol **(B)** Cells treated with TNF- α and 1:250 VCAM-1 primary antibody (Abcam, Waltham, MA 02453) and secondary antibody followed by permeabilization with methanol **(C)** Cells treated with TNF- α and 1:250 VCAM-1 P3C4 primary antibody (Developmental Studies Hybridoma Bank, The University of Iowa, Iowa City, IA) and secondary antibody followed by permeabilization with methanol **(D)** Cells incubated with secondary antibody alone, fixed with 4% paraformaldehyde (PFA), and permeabilized with 0.1% Triton-X **(E)** Cells treated with TNF- α and 1:250 VCAM-1 primary antibody (Abcam, Waltham, MA 02453) and secondary antibody, fixed with 4%PFA, and permeabilized with 0.1% Triton-X **(F)** Cells treated with TNF- α and 1:250 VCAM-1 P3C4 primary antibody (Developmental Studies Hybridoma Bank, The University of Iowa, Iowa City, IA) and secondary antibody, fixed with 4% PFA, and permeabilized with 0.1% Triton-X

4.3 Effect of TNF- α and nanoemulsion (CNEs & SNEs) on insulin signaling:

The hCMEC/D3 cells grown on 6-well plates were incubated with 1% FBS media with and without TNF- α (10ng/ml) for 12 hours followed by 1-hour exposure to 50 μ l of nanoemulsion and finally, the cells were exposed for 20 minutes to 100nm Humulin®. The cells treated with TNF- α , NEs, and Insulin were compared to untreated control cells, cells treated with NEs only, TNF- α , Humulin® only, and TNF- α + Humulin®.

Cells exposed to TNF- α followed by 20 minutes of Humulin® exposure demonstrated a significant decrease in p-AKT/AKT ratio when compared to the Humulin® alone control group. The p-AKT/AKT ratio remained comparable to that of the TNF- α + Humulin® group when the cells were treated with CNEs, possibly demonstrating that saturated fatty acids do not improve the insulin signaling pathway; however, when cells were exposed to SNEs, nanoemulsion with unsaturated fatty acids demonstrated a significant increase in p-AKT/AKT ratio after the cells were exposed to TNF- α and Humulin® in comparison to TNF- α + Humulin® control group. Based on the western blot analysis, the SNEs possibly reversed the reduced insulin signaling due to TNF- α , to levels comparable to that of the Humulin® alone control group (**Fig 10**).

For determining the VCAM-1 expression, the cells grown on the confocal dishes as described above were incubated in 1% FBS media for 12 hours. The treatment dishes were exposed to 12 hours of TNF- α , which includes 1 hour 20 minutes of treatment with 50 μ l of SNEs or CNEs and finally 20 minutes of Humulin® treatment. The dishes with secondary Ab control, untreated control, Humulin® only, CNEs only, and SNEs only (**Fig 11: image A-E**) served as the control dishes.

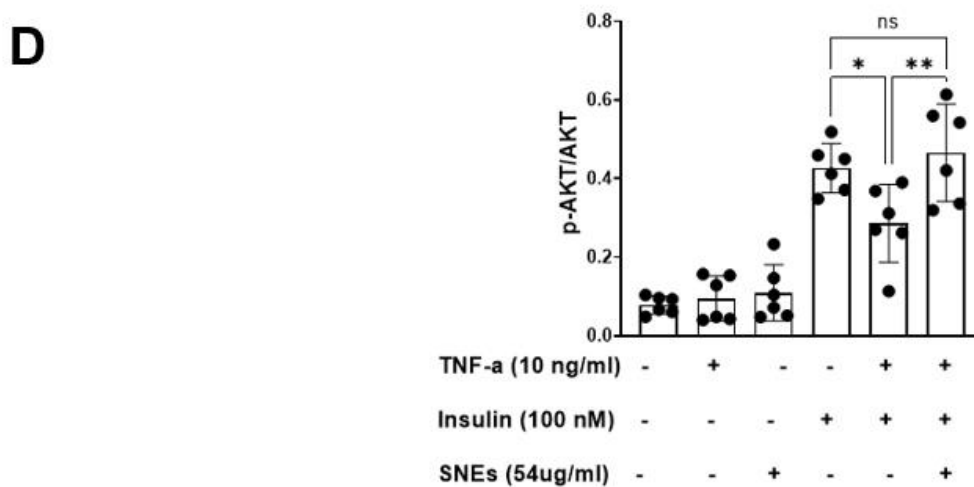
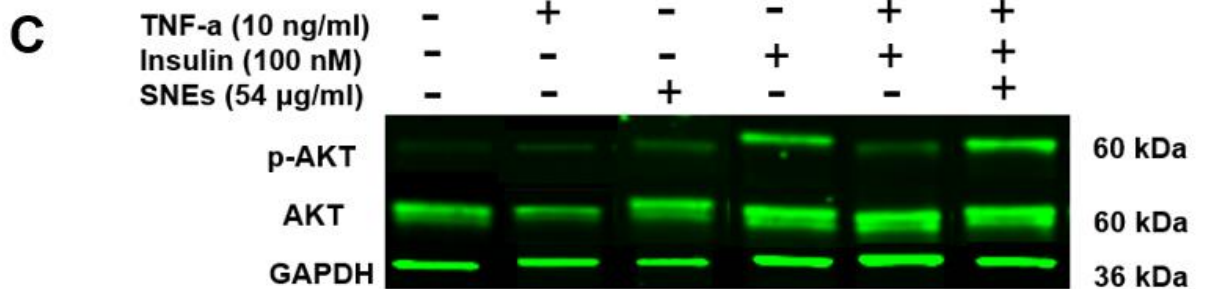
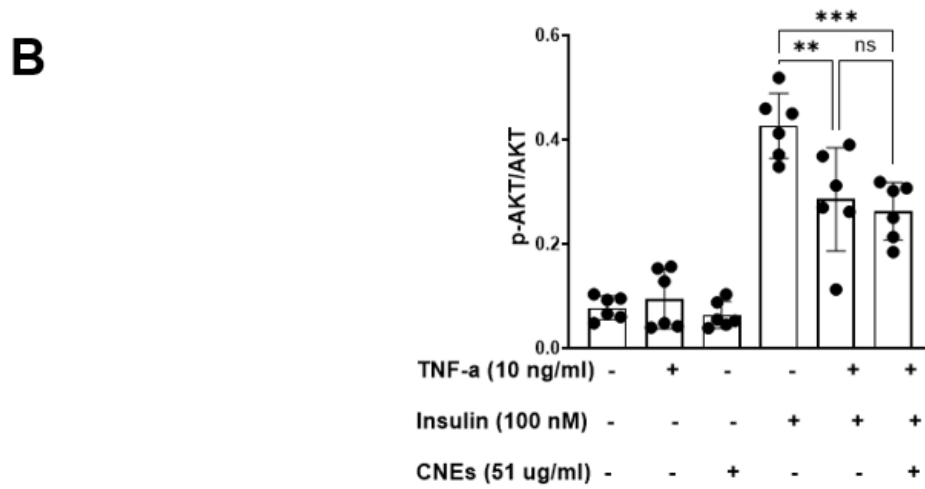
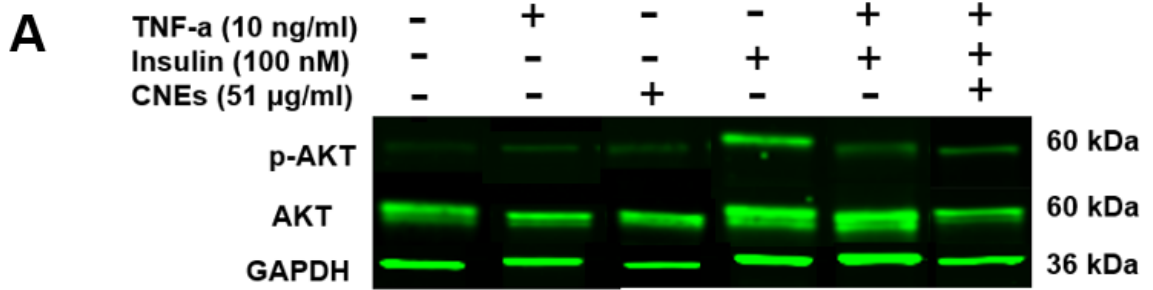


Fig 10: (A) Western blot showing the effect of CNEs on p-AKT and AKT after the cells were exposed to TNF- α and Humulin® **(B)** Quantitation p-AKT/AKT ratios after cells were treated with CNEs, TNF- α and Humulin® **(C)** Western blot showing the effect of SNEs on p-AKT and AKT after the cells were exposed to TNF- α and Humulin® **(D)** Quantitation p-AKT/AKT ratios after cells were treated with SNEs, TNF- α , and Humulin® (One-way ANOVA with Tukey's post-tests, *P<0.05, **P<0.01, ***p<0.001)

It was observed that the cells treated with TNF- α upregulated VCAM-1 expression, a phenomenon which has been well documented (**Fig 11: image F**). It was observed that in presence of Humulin®, the VCAM-1 expression was further upregulated (**Fig 11: image G**), this can be attributed to inhibition of the Pi3K/AKT pathway in the presence of TNF- α and upregulation of p-38MAPK or NF-kB pathway. Additionally, looking into the effect of saturated fatty acids (CNEs) as seen in (**Fig 11: image H**), it was observed that the nanoparticle in combination with TNF- α has the potential to upregulate the VCAM-1 expression and this effect was further amplified when the cells were treated with the triplet combination of TNF- α , CNEs, and Humulin® (**Fig 11: image J**). The upregulation of VCAM-1 seen in **Fig 11: image J** could be correlated to the downregulation of Pi3K/AKT signaling seen in **Fig 10: images A and B, lane 6**. This further confirms the effect insulin resistance can have on VCAM-1, an inflammatory marker.

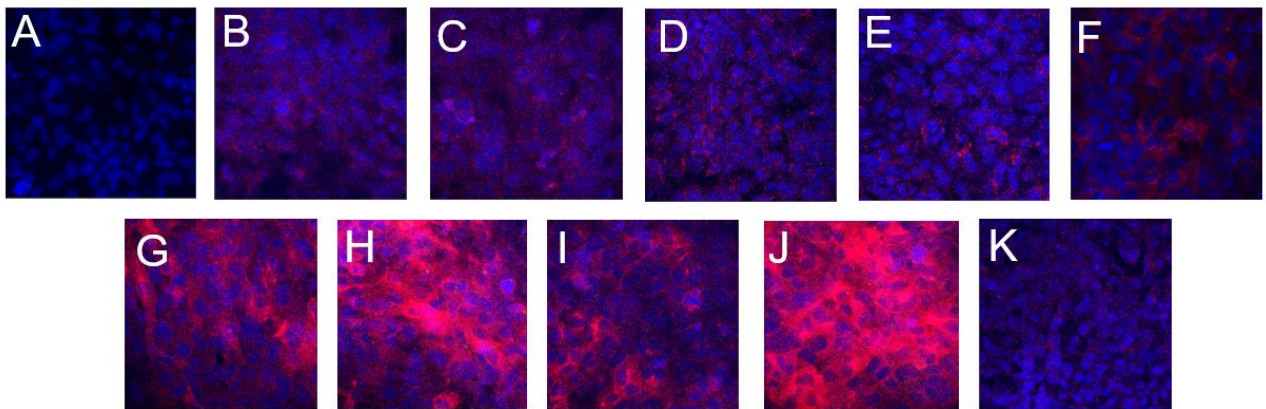


Fig 11: Confocal images for determining VCAM-1 expression upon exposure to various nanoemulsions, TNF- α , and Humulin®. **(A)** Secondary antibody control **(B)** Untreated control **(C)** Humulin® treatment **(D)** Cells treated with CNEs **(E)** Cells treated with SNEs **(F)** Cells treated with TNF- α **(G)** TNF- α + Humulin® **(H)** TNF- α + CNEs **(I)** TNF- α + SNEs **(J)** TNF- α + CNEs+ Humulin® **(K)** TNF- α + SNEs+ Humulin®

Soybean has a greater percentage of unsaturated fatty acids in comparison to coconut oil, the nanoparticle has previously shown the potential to upregulate insulin signaling when combined with Humulin®. This SNEs synergistic effect on insulin signaling was observed even in the presence of TNF- α and Humulin® as seen in **Fig 10: image C and D**. In line with the hypothesis, it was seen that after exposing the cells to TNF- α when cells were treated with SNEs, there was a significant downregulation of VCAM-1 expression (**Fig11: image I**), this could be due to the anti-inflammatory effect of soybean oil due to its unsaturated fatty acids. The effect of soybean oil was further amplified when the cells were treated with Humulin® after treatment with TNF- α and SNEs (**Fig 11: image K**). This can be attributed to the potential activation of the Pi3K/AKT pathway as seen in **Fig 10: image D, lane 6**.

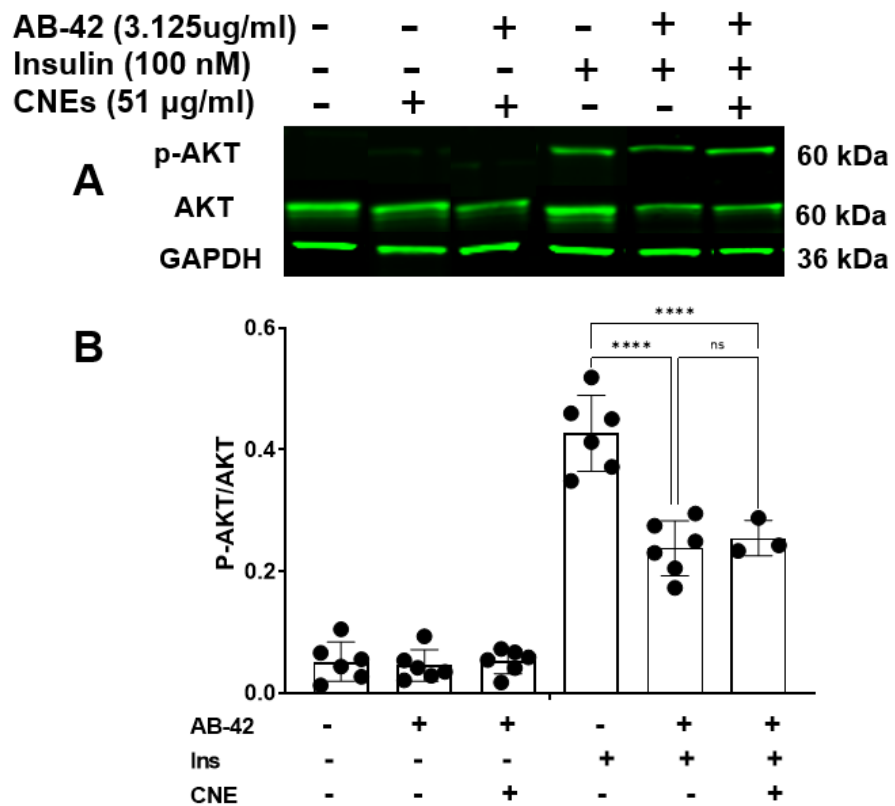
4.4 Insulin resistance and VCAM-1 expression in presence of A β -42 and nanoemulsions:

The hCMEC/D3 cells grown on 6-well plates were incubated with 1% FBS media with for 12 hours followed by a 15-minute exposure to with A β -42 (3.125 μ g/ml) and then the cells were subjected to 1-hour exposure of 50 μ l of nanoemulsion treatment and finally, the cells were exposed to 20 minutes of 100nm Humulin®. The cells treated with A β -42, NEs, and Insulin were compared to untreated control cells, cells treated with NEs only, A β -42 only, Humulin®, and A β -42 + Humulin®.

Cells exposed to A β -42 for 15 mins followed by 20 minutes of Humulin® exposure demonstrated a significant decrease in p-AKT/AKT ratio (**Fig 12**) when compared

to the Humulin® alone control group. The p-AKT/AKT ratio remained comparable to that of the Aβ-42 + Humulin® control group when the cells were treated with CNEs, possibly demonstrating that saturated fatty acids do not affect the insulin signaling pathway in the same magnitude as seen in the case of TNF-α; a similar trend was observed when cells were exposed to SNEs, the p-AKT/AKT ratio remained significantly decreased in comparison to the insulin alone group and the ratio was comparable to Aβ-42 + Humulin® alone group.

This possibly hints towards the possibility that TNF- α and Aβ-42 have a different mechanism by which it affects the insulin signaling pathways or has an effect on the nanoparticle uptake, which could be the reason the NEs do not have a similar effect when cells were exposed to Aβ-42.



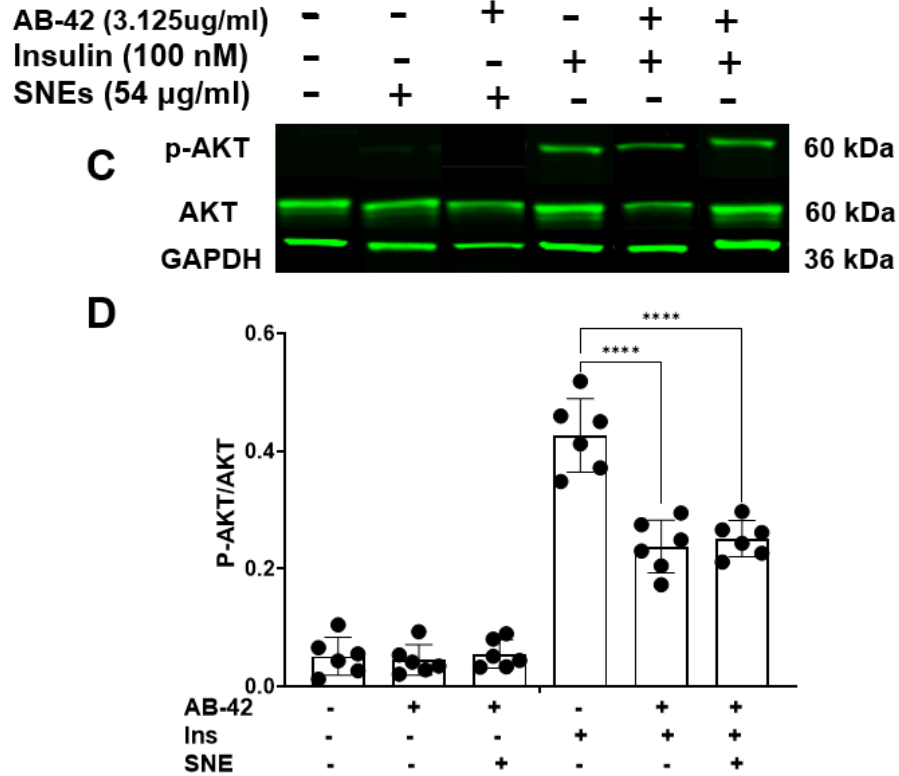


Fig 12: (A) Western blots showing the effect of coconut oil nanoemulsions (CNEs) on p-AKT and AKT after the cells were exposed to A β -42 and Humulin® **(B)** Quantitation of p-AKT/AKT ratio after cells were treated with CNEs, A β -42 and Humulin® **(C)** Western blots showing the effect of coconut oil nanoemulsions (SNEs) on p-AKT and AKT after the cells were exposed to A β -42 and Humulin® **(D)** Quantitation of p-AKT/AKT ratio after cells were treated with SNEs, A β -42 and Humulin® (One-way ANOVA with Tukey's post-tests, ****p<0.0001)

In the case of VCAM-1 expression, cells grown on coverslip bottom dishes followed the same treatment as described above. The secondary Ab control, untreated control, Humulin® only, CNEs only, and SNEs only (**Fig 13: image A-E**) served as the control dishes. There was a noticeable upregulation in VCAM-1 expression when the cells were treated with A β -42 (**Fig13: image F**), the magnitude of upregulation was not as robust as what we observed in the case of TNF- α .

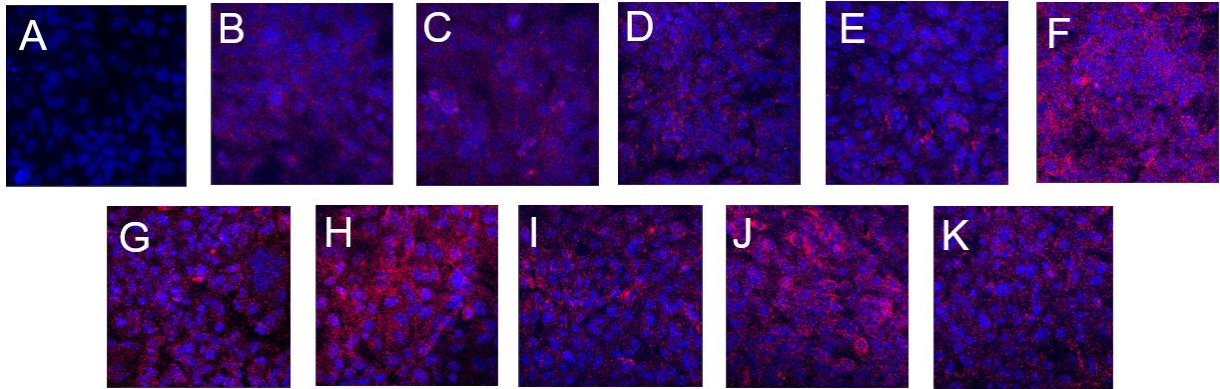


Fig 13: Confocal images for determining VCAM-1 expression in the presence of nanoemulsions (NEs), A β -42, and Humulin®. **(A)** Secondary Ab control **(B)** Untreated control **(C)** Cells treated with Humulin® **(D)** Cells treated with CNEs **(E)** Cells treated with SNEs **(F)** Cells treated with A β -42 **(G)** A β -42+ Humulin® **(H)** A β -42+ CNEs **(I)** A β -42+ SNEs **(J)** A β -42+ CNEs+ Humulin® **(K)** A β -42+ SNEs+ Humulin®

On analyzing the intensity of VCAM-1 expression (**Fig 14**), it was determined that Humulin® did not potentiate A β -42 mediated upregulation of VCAM-1 (**Fig13: image G**). Similarly, when cells were treated with A β -42 and CNEs (**Fig13: image H**), the nanoparticle did not show a similar degree of synergistic effect as it did with TNF- α , however, when compared with SNEs treatment after exposing the cells to A β -42, there was a significant downregulation. (**Fig13: image I**).

One of the possible explanations for this phenomenon could be the result of the short incubation time with A β -42, even though we observe a significant downregulation in p-AKT signaling after 1 hour 35 minutes of total A β -42 exposure. Even though A β -42 can upregulate VCAM-1 expression, it is not as potent as TNF- α , which could mean there could be a delay in the expression of VCAM-1 in the presence of A β -42, increasing incubation time to 3 hours might give us a trend similar to what we observe in the case of TNF- α .

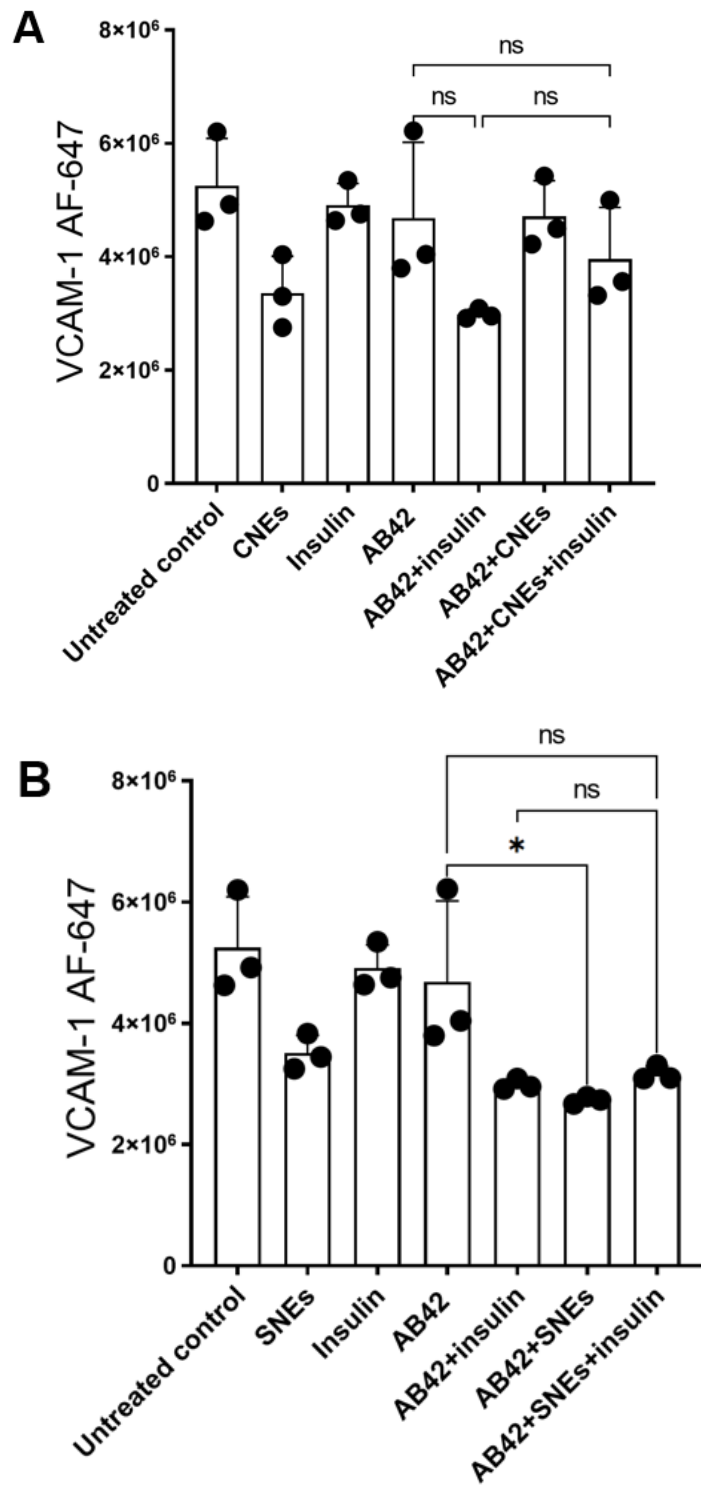


Fig 14: VCAM-1 fluorescence intensities were quantified on Image J and presented as mean \pm SD (One-way ANOVA with Tukey's post-tests, * $P < 0.05$)

4.5 Effect of TNF- α and FNEs on insulin signaling and VCAM-1 expression:

A similar experimental plan was followed for experiments with FNEs. The lipid used (crude fish oil) had 20% to 31% omega-3-fatty acids and \leq 30% of palmitic and stearic acid. To minimize oxidation, α -tocopherol was incorporated into the lipid phase. The hCMEC/D3 cells were grown on 6 well plates and were treated with FNEs after 12-hour incubation with TNF- α followed by 20 minutes of incubation with Humulin®.

Cells exposed to TNF- α followed by 20 minutes of Humulin® exposure demonstrated a significant decrease in p-AKT/AKT ratio when compared to the Humulin® alone control group. There was also a significant reduction in insulin signaling after the cells were treated with FNEs, TNF- α , and Humulin®. (**Fig 15: image A & B**)

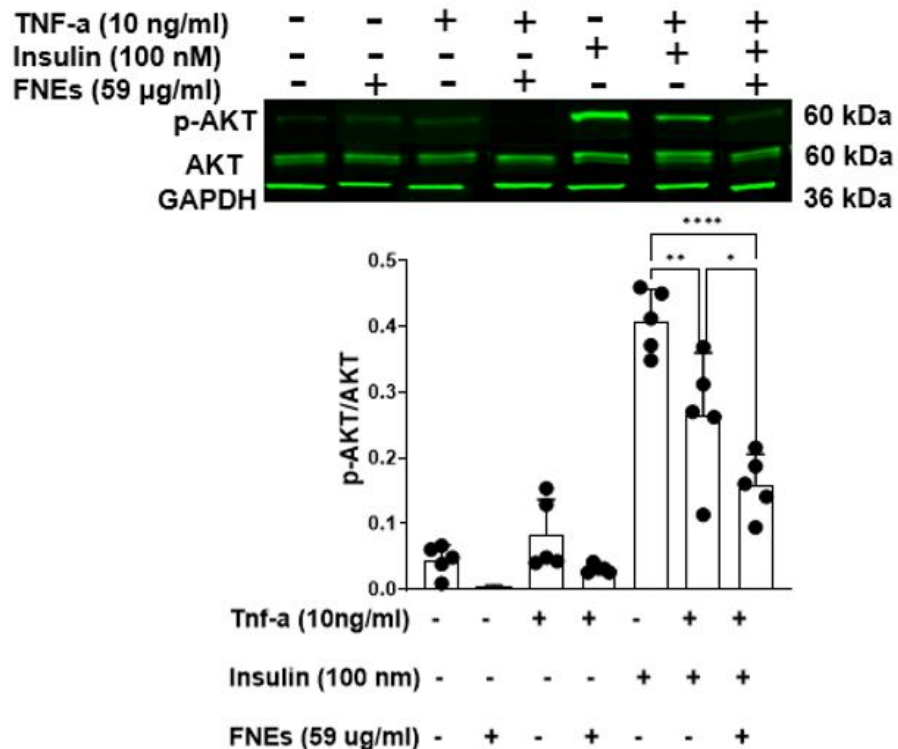
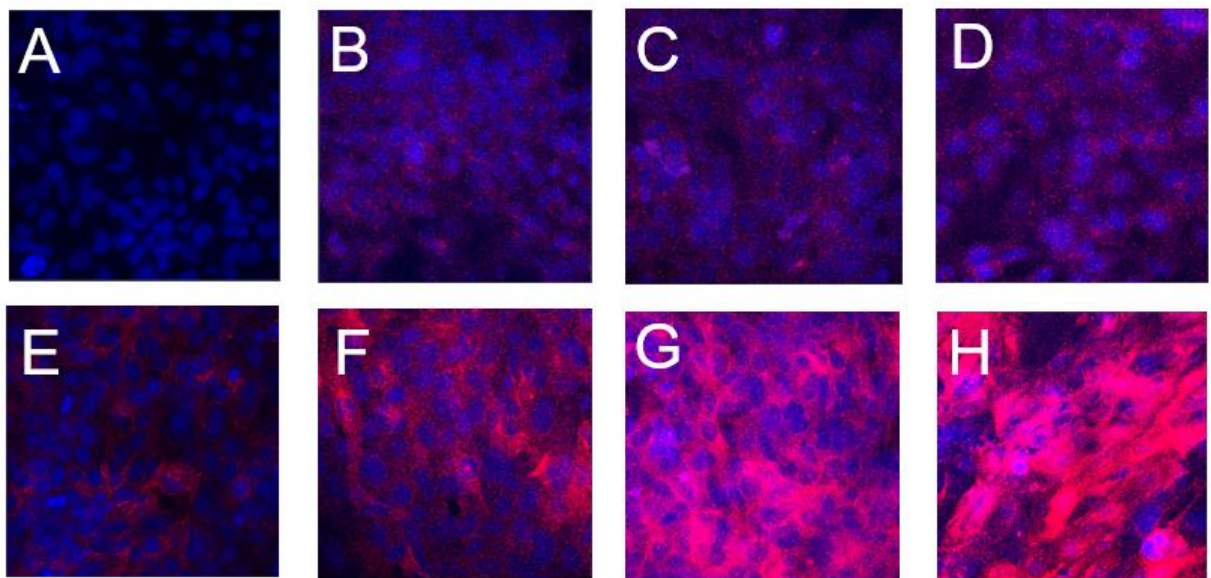


Fig 15: (A) Western showing the effect of fish oil nanoemulsions (FNEs) on p-AKT and AKT after the cells were exposed to TNF- α and Humulin® **(B)** Quantitation of

the p-AKT/AKT ratios after cells were treated with FNEs, TNF- α , and Humulin® (One-way ANOVA with Tukey's post-tests, *P<0.05, **P<0.01, ****p<0.0001)

VCAM-1 expression was determined using confocal microscopy. The dishes secondary ab control, untreated control, Humulin® only, FNEs only, TNF- α only (**Fig16: image A-E**) served as the control dishes. Upregulation of VCAM-1 expression was observed after the cells were treated with TNF- α followed by FNEs (**Fig16: image G**). Similarly, VCAM-1 upregulation was observed after the cells were treated with FNEs, TNF- α , and Humulin® (**Fig16: image H**). The trend observed was similar to what was seen in the case of CNEs (**Fig16: image I**). This confirms the hypothesis that insulin resistance is linked to upregulation of VCAM-1 at the BBB endothelium and the trend becomes further significant when there is lipid dysfunction. The VCAM-1 intensity was analyzed using ImageJ.

One of the possible explanations of this trend could be due to the oxidation of the omega-3-fatty acid resulting in a higher concentration of saturated fatty acids. It might be necessary to optimize the antioxidant concentration to minimize the oxidation and determine the long-term stability of the nanoemulsion.



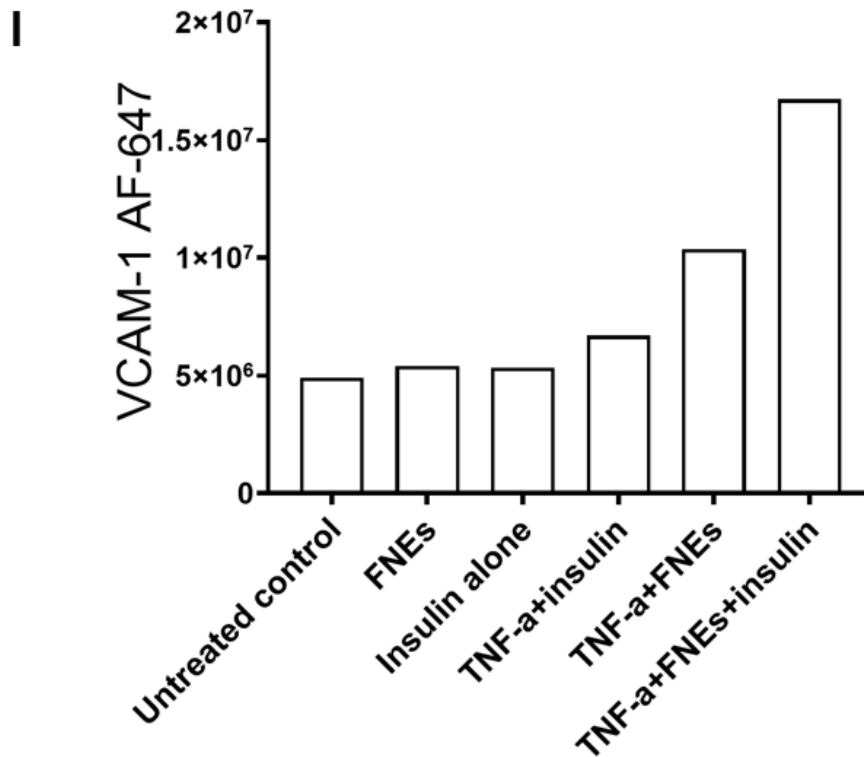


Fig 16: Confocal images of VCAM-1 expression upon treatment with fish oil nanoemulsions (FNEs), TNF- α , and Humulin®. **(A)** Secondary Ab control **(B)** Untreated control **(C)** Cells treated with Humulin® **(D)** Cells treated with FNEs **(E)** Cells treated with TNF- α **(F)** TNF- α + Humulin® **(G)** TNF- α + FNEs **(H)** TNF- α + FNEs+ Humulin® **(I)** Quantification of VCAM-1 fluorescence intensities by Image J and analyzed using GraphPad Prism.

5.0 Discussion:

BBB dysfunction is observed in people suffering from neurological disorders and is considered to be one of the hallmarks of AD. The BBB dysfunction is often associated with a decrease in brain insulin level, an increase in A β deposition, and exacerbated vascular inflammation. Modern-day diets, rich in saturated fats, enhance the AD risk.

The importance of a diet rich in unsaturated fatty acids cannot be understated. Epidemiological evidence and intervention studies clearly show that in humans

saturated fat significantly worsens insulin resistance, while monounsaturated and polyunsaturated fatty acids improve it through modifications in the composition of cell membranes. According to Ohkawa et al., male rats administered with total parenteral nutrition with saturated fat for 4 days, the rats developed hyperglycemia, hyperinsulinemia, and hypotriglyceridaemia. These disorders were mitigated when the rats were given TPN with soybean oil. The study also observed that rats administered with fat-free TPN also developed insulin resistance(52). According to a systematic review and meta-analysis of 102 randomized controlled trials with 4,660 participants concluded that monounsaturated fatty acids (MUFA) improved glycemia and insulin resistance, with the stronger effect seen in patients with T2D; moreover, a diet rich in polyunsaturated fatty acid (PUFA) improved long term glycemic control and insulin signaling in comparison to a diet rich in short-chain fatty acids (SFA) or carbohydrates(57).

The SFAs such as myristic acid (14:0) and Palmitic acid (16:0) etc can activate the proinflammatory cascade mechanism and can induce insulin resistance(57). A study published by Zhao et al. investigated the effect of α -linolenic acid on inflammation and cardiovascular risk in hypercholesterolemic men and women. They demonstrated that a diet rich in PUFA significantly decreased the serum ICAM-1 and E-selectin levels in comparison to SFA; moreover, α -linolenic acid significantly reduced VCAM-1 and E-selectin levels when compared to SFAs(58). It was further established by Madonna et al. that in hyperinsulinemia, insulin can potentiate VCAM-1 expression in human umbilical vein endothelial cells in a concentration-dependent manner. This effect was shown to be even more significant in the presence of PI3K inhibitor, which indicates that under insulin resistance, VCAM-1 expression increased, additionally they also identified with the help of SB-203580 (an inhibitor of the p-38MAPK pathway) there was a downregulation in hyperinsulinemia induced VCAM-1 expression(50). TNF- α has also been known to stimulate all three MAP Kinase, including the p38 MAP Kinases(59). Additionally, In another study that looked at VCAM-1 expression in the presence of TNF- α and Insulin, it is postulated by the author that the synergistic

effect seen with TNF- α and insulin, could be due to TNF- α induced insulin resistance in human umbilical vein endothelial cells(51). This upregulation was determined to be due to NF-kB activation seen in the presence of TNF- α and insulin(51).

In this study we developed different lipid nanoemulsions, to deliver lipids with different degrees of unsaturation. The nanoemulsion formulated according to an established method(49, 60) has a size range of 150-200 nm with the zeta potential ranging from 30-65mV. We induced insulin resistance in polarized hCMEC/D3 monolayers by exposing them to TNF- α and A β -42.

The time-dependent study demonstrated that TNF- α can significantly downregulate insulin signaling and under the insulin resistance conditions, there is a significant upregulation of VCAM-. It confirms the theory that if the Pi3K/AKT signaling pathway is inhibited, and with the potential activation of p-38Mapk or the NF-kB the VCAM-1 expression is further upregulated, and as it is known that TNF- α also upregulates these pathways, there could be a potential synergistic upregulation of these pathways when cells are treated with Humulin® and TNF- α .(50, 61, 62).

We looked into the potential of Lipid nanoemulsions in mitigating inflammation and determined the impact Pi3K/AKT signaling has on the inflammation process. It has been previously established SNEs can upregulate or potentiate the Pi3K/AKT signaling pathway in the presence of insulin, potentially by improving membrane fluidity. The potential of NEs to modulate the insulin signaling pathway was further expanded in the presence of Inflammation mediators like TNF- α and A β -42.

With the help of Western blot analysis, we determined that lipid nanoemulsion containing soybean oil (SNEs) was able to reverse the insulin resistance induced by TNF- α , whereas the lipid emulsion containing coconut oil (CNEs), engendered insulin resistance. In the case of lipid nanoemulsions with fish oil as its lipid component (FNEs), despite it having unsaturated lipids like omega-3-fatty acids, we

observed a similar trend as CNEs. The omega-3-fatty acids like DHA are known to be highly susceptible to oxidation, as we utilized crude fish oil which had close to 30% fatty acids like stearic and palmitic acid, it is possible that the essential unsaturated fatty acids were oxidized, which triggered insulin resistance. In the case of A β -42, we observed a downregulation of insulin signaling, however, none of the nanoemulsions could reverse the insulin resistance. It might be possible that A β -42 affects the insulin signaling pathway via different mechanisms as compared to TNF- α , with TNF- α potentially upregulating the p-38MAPK or NF-kB pathway. The mechanism with A β -42 upregulates VCAM-1 expression and inhibits the insulin signaling pathway is yet to be elucidated, hence it becomes imperative to determine the exact mechanism via which TNF- α and A β -42 induce insulin resistance, additionally, determine an optimal method of formulating fish oil nanoemulsion followed by stability studies for the nanoemulsion could be the potential next steps for this study.

After showing that SNEs have the potential to modulate insulin signaling, we ventured to determine if this effect leads to a reduction in VCAM-1 expression, which is considered a marker for endothelial inflammation. Using laser confocal microscopy, we determined the effect of nanoemulsion exposure on VCAM-1 expression when the cells were under the conditions that triggered insulin resistance. It has been established that TNF- α can significantly upregulate VCAM-1 expression. And when the cells were exposed to Humulin® along with TNF- α , the upregulation was much more prominent, which is in line with the published literature. Nanoemulsions by themselves demonstrated the ability to alter VCAM-1 expression. The coconut oil nanoemulsion (CNEs) had a synergistic effect with TNF- α , thus demonstrating that saturated fatty acids potentially have pro-inflammatory effects. This effect was further upregulated in the presence of Humulin® and TNF- α . However, this trend was reversed when the cells were treated with soybean oil nanoemulsions (SNEs); the VCAM-1 expression was reduced to baseline when the cells were treated with SNEs in the presence of Humulin® TNF- α . This effect is most likely due to improved insulin signaling and

reduced inflammation at the BBB. When the cells were treated with FNEs, we observed a decrease in insulin signaling, which we attribute to the oxidation of essential omega-3-fatty acids and an increase in saturated lipids. Treatment with FNEs and TNF- α further upregulated the VCAM-1 expression.

This highlights the effect of the unsaturated lipids on potentiating insulin signaling as well as mitigating the VCAM-1 expression, which suggests an interaction between the two mechanisms. After determining the underlying mechanisms by which TNF- α and A β -42 induce insulin resistance, the SNE design could be further improved by incorporating appropriate therapeutic agents that can selectively target various kinases in the signaling pathways.

6.0 Conclusion and future plans

6.1 Conclusion

For this study, we formulated 3 lipid nanoemulsions with DOTAP: DPPC in 3:2 ratio w/w. The lipid core of the emulsion differed in the concentration of saturated and unsaturated lipids.

It was established that SNEs could improve insulin signaling after it is significantly downregulated in the presence of TNF- α and insulin, and confocal microscopy demonstrated a significant downregulation of VCAM-1 expression. When CNEs were evaluated, in line with the hypothesis, the nanoemulsion did not upregulate the p-AKT pathway after it was downregulated by TNF- α and insulin. This could be attributed to the percentage of saturated fatty acids present in coconut oil. The role of the Pi3K/AKT pathway became more apparent when the confocal microscopy showed an upregulation of VCAM-1 expression in the presence of TNF- α , CNEs, and insulin.

To further confirm the hypothesis, we formulated fish oil nanoemulsions (FNEs), and to minimize oxidation of fish oil and the anti-inflammatory effect of α -tocopherol we incorporated 0.25% of the antioxidant in the emulsion. The western blot analysis

demonstrated a downregulation of the p-AKT pathway after it was inhibited in the presence of TNF- α and Humulin®. This was attributed to insufficient addition of the antioxidant which would potentially mean oxidation of the essential omega-3-fatty acids. These results, however, helped to further establish the role the Pi3K pathway could be playing in modulating the VCAM-1 expression, as the confocal microscopy demonstrated an upregulation of VCAM-1 expression in the presence of FNEs, TNF- α , and insulin.

When the hypothesis was tested for A β -42, even though there was a significant downregulation of the insulin signaling pathway in the presence of A β -42 and Humulin®. SNEs did not exert the same effect which was seen in the presence of TNF- α , and similarly, the confocal microscopy did not demonstrate significant upregulation of VCAM-1. It could be possible that there is a different pathway by which A β -42 exerts its inflammation effect which could be independent of the Pi3K pathway. However, it should be noted that A β -42 did not significantly upregulate VCAM-1 in comparison to Humulin® alone, which would warrant increasing the incubation time with A β -42 and possibly hints towards a delayed effect in terms of its influence on VCAM-1 expression.

6.2 Future plans

There are still new questions that need to be resolved. The first step would be to resolve the potential oxidation issue encountered with the FNEs by adding different concentrations of antioxidants and by performing stability studies to determine the optimal formulation and then establish the insulin modulatory effect of the fish oil nanoparticle in the presence of Humulin® and finally determine the effect of the nanoemulsion in the modulation of insulin signaling and inflammation in the presence of TNF- α .

Additionally, to resolve the effect of A β -42 on VCAM-1 expression, it becomes imperative to determine the incubation time with the A β -42 and then determine the effect of the nanoemulsion in modulating VCAM-1 expression.

After determining the baseline data we can further expand the study to determine if the insulin resistance and VCAM-1 upregulation is further potentiated if cells are treated with nanoemulsions in the presence of both TNF- α and A β -42.

Finally, we could incorporate lipophilic p-38MAPK inhibitors like Vx745 with SNEs to further resolve the pathways involved in insulin signaling and inflammation at the BBB endothelium.

7.0 Bibliography:

1. Jayaraman A, Pike CJ. Alzheimer's disease and type 2 diabetes: multiple mechanisms contribute to interactions. *Curr Diab Rep.* 2014;14(4):476.
2. Kim B, Feldman EL. Insulin resistance is a key link for the increased risk of cognitive impairment in metabolic syndrome. *Exp Mol Med.* 2015;47:e149.
3. Simons K, Eehalt R. Cholesterol, lipid rafts, and disease. *J Clin Invest.* 2002;110(5):597-603.
4. 2021 Alzheimer's Disease Facts and figures [Internet]. Alzheimers Association. 2021.
5. How Alzheimer's drugs help manage symptoms: Mayo Clinic; 2019 [
6. Jiang T, Yu JT, Tian Y, Tan L. Epidemiology and etiology of Alzheimer's disease: from genetic to non-genetic factors. *Curr Alzheimer Res.* 2013;10(8):852-67.
7. Schachter AS, Davis KL. Alzheimer's disease. *Dialogues Clin Neurosci.* 2000;2(2):91-100.
8. Pike CJ. Sex and the development of Alzheimer's disease. *J Neurosci Res.* 2017;95(1-2):671-80.
9. Alzheimer's Research UK [Internet].
10. FDA Grants Accelerated Approval for Alzheimer's Drug [press release]. fda.gov: FDA2021.
11. Stages of Alzheimer's Disease [Available from: <https://alz.org/alzheimers-dementia/stages>].

12. Abbott NJ, Patabendige AA, Dolman DE, Yusof SR, Begley DJ. Structure and function of the blood-brain barrier. *Neurobiol Dis.* 2010;37(1):13-25.
13. Mulvihill JJ, Cunnane EM, Ross AM, Duskey JT, Tosi G, Grabrucker AM. Drug delivery across the blood-brain barrier: recent advances in the use of nanocarriers. *Nanomedicine (Lond).* 2020;15(2):205-14.
14. Daneman R, Prat A. The blood-brain barrier. *Cold Spring Harb Perspect Biol.* 2015;7(1):a020412.
15. Lindahl P, Johansson BR, Leveen P, Betsholtz C. Pericyte loss and microaneurysm formation in PDGF-B-deficient mice. *Science.* 1997;277(5323):242-5.
16. Wei DC, Morrison EH. Histology, Astrocytes. *StatPearls.* Treasure Island (FL)2022.
17. Sweeney MD, Sagare AP, Zlokovic BV. Blood-brain barrier breakdown in Alzheimer disease and other neurodegenerative disorders. *Nat Rev Neurol.* 2018;14(3):133-50.
18. Akiyama H, Barger S, Barnum S, Bradt B, Bauer J, Cole GM, et al. Inflammation and Alzheimer's disease. *Neurobiol Aging.* 2000;21(3):383-421.
19. Chew H, Solomon VA, Fonteh AN. Involvement of Lipids in Alzheimer's Disease Pathology and Potential Therapies. *Front Physiol.* 2020;11:598.
20. Zlokovic BV. Neurovascular pathways to neurodegeneration in Alzheimer's disease and other disorders. *Nat Rev Neurosci.* 2011;12(12):723-38.
21. Huo H, Guo X, Hong S, Jiang M, Liu X, Liao K. Lipid rafts/caveolae are essential for insulin-like growth factor-1 receptor signaling during 3T3-L1 preadipocyte differentiation induction. *J Biol Chem.* 2003;278(13):11561-9.
22. Simopoulos AP. Human requirement for N-3 polyunsaturated fatty acids. *Poult Sci.* 2000;79(7):961-70.
23. Denis I, Potier B, Vancassel S, Heberden C, Lavalie M. Omega-3 fatty acids and brain resistance to ageing and stress: body of evidence and possible mechanisms. *Ageing Res Rev.* 2013;12(2):579-94.

24. Kanoski SE, Davidson TL. Western diet consumption and cognitive impairment: links to hippocampal dysfunction and obesity. *Physiol Behav.* 2011;103(1):59-68.
25. Andreone BJ, Chow BW, Tata A, Lacoste B, Ben-Zvi A, Bullock K, et al. Blood-Brain Barrier Permeability Is Regulated by Lipid Transport-Dependent Suppression of Caveolae-Mediated Transcytosis. *Neuron.* 2017;94(3):581-94 e5.
26. Eser Ocak P, Ocak U, Sherchan P, Zhang JH, Tang J. Insights into major facilitator superfamily domain-containing protein-2a (Mfsd2a) in physiology and pathophysiology. What do we know so far? *J Neurosci Res.* 2020;98(1):29-41.
27. Holscher C. Insulin Signaling Impairment in the Brain as a Risk Factor in Alzheimer's Disease. *Front Aging Neurosci.* 2019;11:88.
28. Theresa V. Rohm DTM, Jerrold M. Olefsky, Marc Y. Donath. Inflammation in obesity, diabetes, and related disorders. *Immunity.* 2022;55(1):31-55.
29. Uysal KT, Wiesbrock SM, Marino MW, Hotamisligil GS. Protection from obesity-induced insulin resistance in mice lacking TNF-alpha function. *Nature.* 1997;389(6651):610-4.
30. Khan MSH, Hegde V. Obesity and Diabetes Mediated Chronic Inflammation: A Potential Biomarker in Alzheimer's Disease. *J Pers Med.* 2020;10(2).
31. Bedse G, Di Domenico F, Serviddio G, Cassano T. Aberrant insulin signaling in Alzheimer's disease: current knowledge. *Front Neurosci.* 2015;9:204.
32. Zenaro E, Piacentino G, Constantin G. The blood-brain barrier in Alzheimer's disease. *Neurobiol Dis.* 2017;107:41-56.
33. Wennstrom M, Nielsen HM. Cell adhesion molecules in Alzheimer's disease. *Degener Neurol Neuromuscul Dis.* 2012;2:65-77.
34. Drake JD, Chambers AB, Ott BR, Daiello LA, Alzheimer's Disease Neuroimaging I. Peripheral Markers of Vascular Endothelial Dysfunction Show Independent but Additive Relationships with Brain-Based Biomarkers in Association with Functional Impairment in Alzheimer's Disease. *J Alzheimers Dis.* 2021;80(4):1553-65.

35. Yamagishi K, Ikeda A, Chei CL, Noda H, Umesawa M, Cui R, et al. Serum alpha-linolenic and other omega-3 fatty acids, and risk of disabling dementia: Community-based nested case-control study. *Clin Nutr.* 2017;36(3):793-7.
36. Thomas J, Thomas CJ, Radcliffe J, Itsiopoulos C. Omega-3 Fatty Acids in Early Prevention of Inflammatory Neurodegenerative Disease: A Focus on Alzheimer's Disease. *Biomed Res Int.* 2015;2015:172801.
37. Ajith TA. A Recent Update on the Effects of Omega-3 Fatty Acids in Alzheimer's Disease. *Curr Clin Pharmacol.* 2018;13(4):252-60.
38. Wong D, Dorovini-Zis K. Expression of vascular cell adhesion molecule-1 (VCAM-1) by human brain microvessel endothelial cells in primary culture. *Microvasc Res.* 1995;49(3):325-39.
39. Dong X. Current Strategies for Brain Drug Delivery. *Theranostics.* 2018;8(6):1481-93.
40. Tayeb HH, Felimban R, Almaghrabi S, Hasaballah N. Nanoemulsions: Formulation, characterization, biological fate, and potential role against COVID-19 and other viral outbreaks. *Colloid Interface Sci Commun.* 2021;45:100533.
41. Nur Haziqah Che Marzuki RAW, Mariani Abdul Hamid. An overview of nanoemulsion: concepts of development and cosmeceutical applications. *Biotechnology & Biotechnological Equipment.* 2019;33:779-97.
42. Valéria Maria de Oliveira Cardoso BJM, Edson José Comparetti, Isabella Sampaio, Leonardo Miziara Barboza Ferreira, Paula Maria Pincela Lins and Valtencir Zucolotto*. Is Nanotechnology Helping in the Fight Against COVID-19? *Frontiers.* 2020.
43. K. Gurpreet SKS. Review of Nanoemulsion Formulation and Characterization Techniques. *Indian Journal of Pharmaceutical Sciences.* 2018.
44. Zhang B, Zhou X, Miao Y, Wang X, Yang Y, Zhang X, et al. Effect of phosphatidylcholine on the stability and lipolysis of nanoemulsion drug delivery systems. *Int J Pharm.* 2020;583:119354.
45. Cheng Qian David JM. Formation of nanoemulsions stabilized by model food-grade emulsifiers using high-pressure homogenization: Factors affecting particle size. *Food Hydrocolloids.* 2011;25(5):1000-8.

46. Weller J, Budson A. Current understanding of Alzheimer's disease diagnosis and treatment. *F1000Res*. 2018;7.
47. ADUHELM (aducanumab-avwa) for the Treatment of Alzheimer's Disease [press release]. *Clinical Trials Arena*2021.
48. Yan L, Xie Y, Satyanarayanan SK, Zeng H, Liu Q, Huang M, et al. Omega-3 polyunsaturated fatty acids promote brain-to-blood clearance of beta-Amyloid in a mouse model with Alzheimer's disease. *Brain Behav Immun*. 2020;85:35-45.
49. Lushan Wang, Timothy Wiedmann, Karunya Kandimalla. Modulating Insulin Signaling and Trafficking in the Blood Brain Barrier Endothelium Using Lipid Based Nanoemulsions. [Thesis]. In press 2022.
50. Madonna R, Pandolfi A, Massaro M, Consoli A, De Caterina R. Insulin enhances vascular cell adhesion molecule-1 expression in human cultured endothelial cells through a pro-atherogenic pathway mediated by p38 mitogen-activated protein-kinase. *Diabetologia*. 2004;47(3):532-6.
51. Madonna R, Massaro M, De Caterina R. Insulin potentiates cytokine-induced VCAM-1 expression in human endothelial cells. *Biochim Biophys Acta*. 2008;1782(9):511-6.
52. Ohkawa H, Fukuwa C, Matsuzawa-Nagata N, Yokogawa K, Omura K, Miyamoto K. Soybean fat supplementation controls insulin resistance caused by fat-free total parenteral nutrition. *J Pharm Pharmacol*. 2008;60(4):461-5.
53. Vrishali Salian, Val J. Lowe, Karunya K. Kandimalla, Geoffry L. Curran, Decklever T. Molecular Mechanisms of Cerebrovascular Inflammation in Alzheimer's Disease. *American Association of Pharmaceutical Scientists*2020.
54. Durmus M. Fish oil for human health: omega-3 fatty acid profiles of marine seafood species. *Scielo Brazil*. 2019.
55. Clemente TE, Cahoon EB. Soybean oil: genetic approaches for modification of functionality and total content. *Plant Physiol*. 2009;151(3):1030-40.
56. Boateng L, Ansong R, Owusu WB, Steiner-Asiedu M. Coconut oil and palm oil's role in nutrition, health and national development: A review. *Ghana Med J*. 2016;50(3):189-96.

57. Imamura F, Micha R, Wu JH, de Oliveira Otto MC, Otite FO, Abioye AI, et al. Effects of Saturated Fat, Polyunsaturated Fat, Monounsaturated Fat, and Carbohydrate on Glucose-Insulin Homeostasis: A Systematic Review and Meta-analysis of Randomised Controlled Feeding Trials. *PLoS Med.* 2016;13(7):e1002087.
58. Zhao G, Etherton TD, Martin KR, West SG, Gillies PJ, Kris-Etherton PM. Dietary alpha-linolenic acid reduces inflammatory and lipid cardiovascular risk factors in hypercholesterolemic men and women. *J Nutr.* 2004;134(11):2991-7.
59. Sabio G, Davis RJ. TNF and MAP kinase signalling pathways. *Semin Immunol.* 2014;26(3):237-45.
60. T. Vladislavljević G. Preparation of microemulsions and nanoemulsions by membrane emulsification. *Colloids and Surfaces A: Physicochemical and Engineering Aspects.* 2019;579.
61. Pott GB, Tsurudome M, Bamfo N, Goalstone ML. ERK2 and Akt are negative regulators of insulin and Tumor Necrosis Factor-alpha stimulated VCAM-1 expression in rat aorta endothelial cells. *J Inflamm (Lond).* 2016;13:6.
62. Kumphune S, Chattipakorn S, Chattipakorn N. Roles of p38-MAPK in insulin resistant heart: evidence from bench to future bedside application. *Curr Pharm Des.* 2013;19(32):5742-54.